3-11-2011

# Characterization of Graphite Composite Material Particulates from USAF Aircraft Maintenance Operations

Richard E. Yon


# CHARACTERIZATION OF GRAPHITE COMPOSITE MATERIAL PARTICULATES FROM UNITED STATES AIR FORCE AIRCRAFT MAINTENANCE OPERATIONS

THESIS

Richard E. Yon, Captain, USAF, BSC

AFIT/GIH/ENV/11-M04

**DEPARTMENT OF THE AIR FORCE**
**AIR UNIVERSITY**

## AIR FORCE INSTITUTE OF TECHNOLOGY

**Wright-Patterson Air Force Base, Ohio**

AFIT/GIH/ENV/11-M04

# CHARACTERIZATION OF GRAPHITE COMPOSITE MATERIAL PARTICULATES FROM UNITED STATES AIR FORCE AIRCRAFT MAINTENANCE OPERATIONS

THESIS

Presented to the Faculty

Department of Systems and Engineering Management

Graduate School of Engineering and Management

Air Force Institute of Technology

Air University

Air Education and Training Command

In Partial Fulfillment of the Requirements for the

Degree of Master of Science in Industrial Hygiene

Richard E. Yon, BS

Captain, USAF, BSC

March 2011

AFIT/GIH/ENV/11-M04

# CHARACTERIZATION OF GRAPHITE COMPOSITE MATERIAL PARTICULATES FROM UNITED STATES AIR FORCE AIRCRAFT MAINTENANCE OPERATIONS

Richard E. Yon, BS
Captain, USAF, BSC

Approved:

| | |
|---|---|
| //signed// | 4 Mar 2011 |
| Lt Col Dirk P. Yamamoto (Chairman) | Date |
| //signed// | 25 Feb 2011 |
| Lt Col Jeremy M. Slagley (Member) | Date |
| //signed// | 25 Feb 2011 |
| Daniel L. Felker, PhD (Member) | Date |

# Abstract

Due to their benefits of light weight, high strength and stiffness, and adaptable material properties, advanced composite materials (ACM) are increasingly being used as structural components on aircraft, especially within the United States Air Force: C-17 (8% by weight), B-2 (37%), F-22 (38%), and F-35 (39%). As a result, the potential exists for occupational exposures to structural maintenance employees while repairing and fabricating aircraft components. Two field studies were conducted for this thesis in order to characterize ACM aerosol size distribution, determine the feasibility of utilizing direct reading instruments (DRIs) in the field, and ensure workers are protected with adequate controls. In order to characterize exposure, traditional integrated air sampling (NIOSH Methods 0500, 0600, 7400 and 5040) and DRIs were positioned together near an ACM panel as it was cut with a core milling machine. Gravimetric analyses and fiber counts were conducted on the integrated samples, whereas particle counts and size distributions were analyzed using the DRIs (optical and condensation particle counters). Statistics reveal a significant decrease ($p$-value $< 0.0001$) in the particle count for respirable sized ultra-fine particles when the local exhaust ventilation was turned on. The second field study involved utilizing the DRIs during a C-17 crash and recovery operation, which confirmed they can be helpful for base-level bioenvironmental engineers (BEEs) for recommending personal protective equipment for the clean-up crew. The results of this research suggest that the combination of an OPC and a CPC enable the creation of one particle size distribution that can be used for ensuring adequacy of engineering controls.

# Acknowledgments

I want to express my gratitude to Lt Col Jeremy Slagley, who began as my advisor and greatly enhanced my learning while at AFIT. To Lt Col Yamamoto, who graciously took over as advisor: thank you for challenging me and steering me in the right direction. My thanks extend to Dr. Felker for his patience when I asked him the same questions over and over as I tried to learn how the Scanning Electron Microscope works; your guidance and direction for my research have been invaluable.

A special token of appreciation goes out to the United States Air Force School of Aerospace Medicine for providing financial support, equipment and supplies to gather the necessary data for my thesis research. I appreciate the knowledge and assistance of Capt Ferreri and Capt Horenziak, who helped me on gathering the data during the field studies.

I would like to thank the Lord for helping me through the Industrial Hygiene graduate course and for keeping me sane and focused during my research and writing of this thesis. Surely, I would not have been able to accomplish this endeavor without the love and support of my wife and the rest of my family. I would like to give a special thanks to all who prayed for me and encouraged me along the way.

Richard E. Yon

# Table of Contents

**Page**

# List of Figures

# List of Tables

CHARACTERIZATION OF GRAPHITE COMPOSITE MATERIAL PARTICULATES FROM UNITED STATES AIR FORCE AIRCRAFT MAINTENANCE OPERATIONS

# I. Introduction

Due to their benefits of light weight, high strength and stiffness, and adaptable material properties, advanced composite materials (ACM) are increasingly being used as structural components on aircraft, especially within the United States Air Force. As a result, structural maintenance employees may potentially be exposed to these materials while repairing and fabricating aircraft components. Airframes containing ACM include C-17 (8% by weight), B-2 (37%), F-22 (38%), and F-35 (estimated 35% structural weight and most of visible skin surfaces). In addition, there have been reports aircraft being retrofitted with ACM upgrades as components are replaced during phase maintenance and inspections (Boeing, 2005).

Other operations that may expose workers to ACM particulate matter include performing maintenance tasks on downed aircraft that may contain burned ACM components, or on battle damaged aircraft (Ferreri, 2010). However, the primary focus of this study is to determine the extent of possible ACM exposure from routine structural maintenance operations throughout Air Force installations.

Studies performed on dermal exposure routes determined that ACM particles may have a sensitizing effect and are possibly linked to dermatitis in maintenance workers (Gandhi, Lyon, & Speitel, 1999). There have been few epidemiological studies on characterizing inhalation exposure risk to ACM particles. However, it has been reported that particle diameter sizes in the 3-5 micron range may easily become airborne and pose

a respirable hazard similar to that of fiberglass (Agency for Toxic Substances and Disease Registry, 2002).

The majority of the ACM fabrication occurs at depot level installations, such as Hill AFB, UT. However, as ACM prevalence on aircraft increases, the potential for workers at base level to perform maintenance on ACM increases. This thesis presents a field study on the characterization of ACM aerosols during graphite-epoxy panel fabrication, or more specifically, the cutting of the ACM panel with a core mill. Area sampling of particulate matter at the point of cutting is utilized to create particle size distributions for exposure potential of employees performing fabrication tasks, such as cutting and grinding.

## Problem Statement

The "gold standard" for performing an exposure assessment on aerosols in industrial hygiene is to collect particulate matter on filter media, conduct gravimetric analysis on the collected mass, and correlate the results with published standards. There are currently no published standards for ACM particulate matter and aerosolized particles generally do not produce enough mass for gravimetric analysis to be useful in exposure characterization, if compared to nuisance dust standards.

Technology is improving in the area of utilizing direct reading instruments (DRIs) for measuring size and concentration of particulate matter. The intent of this thesis is to demonstrate the effectiveness of DRIs in field settings, in hope of increasing the industrial hygienist's confidence in the reliability and usefulness in the DRIs. This will allow base level bioenvironmental engineers (BEEs) the capability of obtaining real-time

ACM aerosol data during occupational operations and aircraft crash responses, allowing for an immediate initial evaluation for the purpose of recommending personal protective equipment. A secondary important aspect of DRI usage is the ability to store and maintain the data for future research and exposure assessment in the event standards are published.

## Research Objectives

The objectives of this thesis are:

1. Characterize the size distribution of aerosolized particulate matter during fabrication of graphite-epoxy composite materials on B-2 panels, as well as crash and recovery operations on a C-17

2. Examine the feasibility of BEEs utilizing direct reading instruments at base-level to perform sampling and analysis for advanced composite materials

3. Ensure that current engineering controls and personnel protective equipment are adequate for workers

# II. Literature Review

Research on advanced composite materials is extensive and may cover many broad areas. Typical composite materials found on aircraft in the U.S. Air Force include boron and carbon fibers having a diameter of 7-10 μm (Ferreri, 2010). The focus of this thesis is on graphite-epoxy composites, which are used on the B-2 and C-17.

The terms graphite and carbon are often used interchangeably, but the difference between them is the purity of the material and the temperature of pyrolysis, which is the manufacturing process of creating the high strength fiber. Graphite fibers are approximately 99 percent carbon, whereas carbon fibers are typically 80-95 percent carbon. In pyrolysis, the polyacrylonitrile (PAN) yarn is burned at a temperature up to 3000 °C, which graphitizes the material and turns it black; carbon fibers are carbonized at temperatures near 1500 °C (Kalpakjian & Schmid, 2001).

The Occupational Safety and Health Administration (OSHA) Technical Manual (OTM) states that there is no health concern with the graphite fibers since they are inert, but the epoxy may pose a dermal hazard, such as allergic dermatitis on skin and conjunctivitis in the eyes (Occupational Safety & Health Administration, 1999). The paragraphs that follow document reviews of the toxicity of particulate matter, ultrafine particles, carbon fibers and nanomaterials.

## Toxicity of Airborne Particulate Matter

Particulate matter that has the potential to become aerosolized during fabrication processes, such as drilling, grinding and cutting, are generally categorized by size and shape. The particles usually have the same chemical properties as the parent material,

until they become small enough in the nanometer range and begin to exhibit different properties and toxic effects. Toxicity of the particulate matter depends on its size and the potential location in the respiratory system that it will be deposited. Because the size of the particle is described by its diameter, and there is a huge band of particle sizes being aerosolized from the material being fabricated, a size distribution needs to be generated as a means of characterization (Hinds, 1999).

Particles larger than 10 µm are deposited in the nasal pathway and are considered non-respirable. Ingestion may also be a route of exposure for particles small enough to pass through the upper respiratory (tracheobronchial) region, by means of mucociliary escalator transport which allows particles to be swallowed (McClellan, 2002). Lung penetration and deposition of aerosol particles in the respiratory system is modeled by the International Standards Organization (ISO, 1995). The model illustrates a 50 percent probability of inhaling particles that are 100 µm or less in diameter, and the probability quickly increases with decreasing particle size. The respirable curve displays the penetration for the particle size of primary concern, 4 µm cut point; that is, there is a 50% probability for particles that are capable of reaching deep into the alveolar region of the lung (Maynard & Kuempel, 2005).

Particles in the size range of 2.5 µm to 10 µm are called coarse particulate matter, and particles less than 2.5 µm are considered fine particulate matter (Li, et al., 2003). Ultrafine particles are those that are smaller than 100 nm, which are common in anthropogenic materials (carbon nanotubes) and processes, such as fabrication operations (Brown, et al., 2003). Ferreri, et al., demonstrated that the cutting of advanced composite material can produce such ultrafine particles (Ferreri, Slagley, & Felker, 2009).

Epidemiological studies, primarily air pollution studies, have linked fine and coarse particulate matter to biological effects such as cardiovascular disease, respiratory illness, chronic obstructive pulmonary disease (COPD) and asthma (Brunekreef & Forsberg, 2005) (Araujo & Nel, 2009) (Puett, et al., 2009). LeBlancab, et al., investigated health effects with various size particles, including fine and ultrafine particulate matter and stated that risk exists for cardiovascular disease, mortality, and myocardial infarction when exposed to fine particulates (LeBlancab, et al., 2009). Their hypothesis was that if fine particulate matter had the aforementioned effects, it is suspected that nanoparticles would have even more harmful effects along the same line, due to the increased pulmonary deposition. Exposing rats to titanium dioxide ($TiO_2$) nanoparticles via inhalation resulted in endothelium-dependent arteriolar vasodilation and produced a negative effect on coronary arterioles (LeBlancab, et al., 2009).

The EPA and ACGIH publish standards for particulate matter based on air pollution and occupational health studies. However, there are not any published standards yet for exposure to carbon fibers, or particulates aerosolized during fabrication of advanced composite materials, which tend to fall into the ultrafine and nanoparticle size range. Currently, it is up to the occupational health specialist to utilize professional judgment in determining engineering controls and personnel protective equipment to ensure the health of employees are protected. Toxic health effects of ultrafine particles will be covered in the following section.

## Ultrafine Particle and Nanoparticle Toxicity

Over the past decade, extensive research has been conducted on the health effects of ultrafine particles and nanoparticles, especially as a result of the increased use of nanomaterials, such as carbon nanotubes. Because ultrafine particles are so small (i.e., small enough to penetrate deep into the alveolar region of the lungs), they have a vital role in the realm of environmental and occupational health regarding particulate matter (Oberdörster & Utell, 2002) (Oberdörster G. , 1996). Li, et al., demonstrated that ultrafine particles are more harmful than fine or coarse particles because they induce oxidative stress at the cellular level, damaging mitochondria and cell membrane (Li, et al., 2003). Oberdörster also reported on the cellular effects of oxidative stress due to ultrafine particle exposure, as it affects cell signaling pathways (Oberdörster, Oberdörster, & Oberdörster, 2005).

These toxicological studies aid in linking biological responses with key factors of particulate matter, such as size, shape, surface area and surface chemistry, which also have an effect on the deposition of particles in the respiratory system (Maynard & Kuempel, 2005) (Oberdörster, et al., 2005). Particulate matter that ends up deep in the lungs has the potential to cause inflammation, cell and tissue damage, and respiratory disease (Donaldson, Li, & MacNee, 1998). Oberdörster also revealed that particulate matter deposited in the nasal area may travel up the olfactory nerve to the olfactory bulb in the brain, which is the sensory receptor for distinguishing odors (Oberdörster, et al., 2004). Studies show that nanometer-sized particles tend to follow the respiratory airstream and are not affected by settling and inertial behaviors that larger, heavier particles follow (Maynard & Kuempel, 2005).

Ultrafine particles have a large surface area-to-mass ratio and commonly agglomerate to form a larger clump of particles, affecting deposition in the respiratory system. Many reports indicate that surface area is a key factor in determining the biological significance of nanoparticles. Sager and Castranova conducted a study to test whether surface area or mass is the proper metric to utilize for pulmonary toxicity studies. They exposed rats to ultrafine and fine carbon black via intratracheal instillation, where particles are directly injected into the lungs through the trachea, as opposed to allowing for the process of inhaling the particles. Surface area and mass of particles were compared to inflammatory and cytotoxic responses. Their results showed that responses were 65 times greater for ultrafine particles than for fine particles, in regards to analysis by mass. However, when the doses were normalized by particle surface area, ultrafine particle inflammatory and cytotoxic responses were only marginally greater than that of fine particles. The study concluded by stating particle surface area may be more appropriate to use than mass when conducting toxicity tests for nanoparticles with low solubility and low toxicity (Sager & Castranova, 2009).

Maynard and Kuempel agree with other researchers that particle size and surface area are the key parameters, rather than mass concentration, when correlating biological responses and determining health risk. Gravimetric analyses are generally not useful for ultrafine particles due to insignificant mass, but may serve as a bridge for establishing standards and new techniques. Although size and surface area are key factors, it is better to obtain a comprehensive characterization of exposure that also includes surface chemistry and morphology of the particles "before and after deposition." (Maynard & Kuempel, 2005)

The increased surface area of ultrafine particles, with a higher composition of carbon than fine and coarse particulate matter, have a greater probability of collecting volatile organic compounds (VOC) that are inclined to travel with the particles to the lungs and contribute to an increased biological response (Li, et al., 2003). The nanoparticle becomes a vessel for carrying the VOC to its target organs, as shown by some studies in associating ultrafine particulate matter with cardiovascular disease (Oberdörster, Oberdörster, & Oberdörster, 2005). Polyaromatic hydrocarbons (PAH) have been known to adsorb onto nanoparticles and enhance their biological potency by inducing reactive oxygen species (ROS) and generating free radicals that cause adverse health effects (Li, et al., 2003). This ROS inducing mechanism has been reported as promoting atherosclerosis, which is a vascular inflammatory disease where lipids build up along the interior of the artery wall (Araujo & Nel, 2009).

In determining absorption and systemic effects, much of the research on dermal effects of nanomaterials indicate that nanoparticles, such as ultrafine-$TiO_2$, do not produce dermal sensitization or irritate the skin (Warheit, et al., 2007). Lademann, et al., experimented with $TiO_2$ nanoparticles within sunscreen on human skin and concluded that particles were not discovered in the epidermal tissue beneath the stratum corneum, but small concentrations were noticed in the lower part of the hair follicles (Lademann, et al., 1999). In contrast, Tinkle, et al., demonstrated that ultrafine berrylium particles (less than 1 μm) are capable of penetrating the stratum corneum and moving into the epidermis in conjunction with motion, such as flexing or twisting of the skin, and may attribute to skin sensitization (Tinkle, et al., 2003).

## Carbon Fiber and Carbon Nanotube Toxicity

Fibers, by definition in health toxicity studies, are particles that have a length-to-diameter ratio greater than three (L/D>3) (Ness, 1991). According to Ghandi, et al., the primary exposure pathways for carbon fibers are inhalation and dermal (Gandhi, Lyon, & Speitel, 1999). Carbon fibers of diameters greater than 4-5 µm have the potential to cause abrasion hazards, break the skin, and cause temporary irritation that is expected to fully recover. Short-term dermatitis and skin irritation are possible from fiber abrasion and punctures of broken fibers (Gandhi, Lyon, & Speitel, 1999). Fibers greater than 7-10 µm are too large to reach the deep lung and do not pose an inhalation hazard, but those fibers less than 3 µm have the capability of aligning themselves with the airstream and penetrating into the alveolar region of the lung (Gandhi, Lyon, & Speitel, 1999).

In the proceedings of a carbon fiber toxicology conference in 1989, Thomson indicated that animal studies on carbon fibers resulted in only temporary dermal irritations and upper respiratory health effects, demonstrating that there is no long-term health risk associated with occupational exposure to carbon fibers greater than 6 µm (Thomson, 1989). Warheit et al. exposed rats to carbon fibers with a mean diameter of 4.4 µm, which resulted in a minor inflammatory response in the lungs, but the effects reversed ten days later (Warheit, Hansen, Carakostas, & Hartsky, 1994).

Studies show that machining advanced composite materials creates aerosols containing a small fraction of carbon fibers of 7-11 µm in diameter and nonfibrous particulates with an average diameter of 2.7 µm. Martin et al. captured such aerosol particulates and directly inserted them into lungs of rats by intratracheal injection (Martin, Meyer, & Luchtel, 1989). Their results revealed low to moderate level lesions

and inflammation in the lung tissue; however, they concluded that the composite particulate matter should be treated as nuisance dust (Martin, Meyer, & Luchtel, 1989). The National Institute for Occupational Safety and Health (NIOSH) refers to this nuisance dust as particles not otherwise specified or regulated, PNOS or PNOR (NIOSH, 2010).

## NIOSH NEAT Method

The NIOSH nanotechnology field research team developed the Nanoparticle Emission Assessment Technique (NEAT), in order to aid in examining worker exposure to aerosolized nanoparticles, specifically where nanomaterials are produced and handled (Methner, Hodson, & Geraci, 2010). The NEAT method may prove to be useful in other aerosol field studies as well, in order to determine if nano-sized particulates may become airborne, such as during the fabrication of advanced composite materials and cutting up downed aircraft containing ACM. The method is used to evaluate the concentration of airborne particulate matter. It is not an exact quantitative measurement, but the use of direct reading instruments does aid in identifying source emissions, enabling the occupational health professional to make immediate recommendations on personal protective equipment.

The direct reading instruments utilized in the NEAT method are an optical particle counter (OPC) and a condensation particle counter (CPC), which are used in combination and in conjunction with conventional filter-based air sampling methods. The filter media used to collect air samples can then be analyzed with an electron

microscope for determining the identity and chemical structure of the nanoparticles. The OPC and CPC are generally handheld and portable, allowing for a useful means of identifying operations and sources that potentially lead to the increase of airborne nano-sized particulate matter (Methner, Hodson, & Geraci, 2010). Ferreri's research on characterizing burnt carbon composite material entailed a similar approach to evaluate a bench top experiment with the NEAT method (Ferreri, 2010).

The NIOSH nanotechnology field research team set out to perform actual field occupational health studies to characterize processes that have the potential to expose workers to nanomaterials; to evaluate these potential exposures with several measurement methods; to determine if existing controls are adequate; and to recommend safe and healthy work practices (Methner, et al., 2010). The team performed 12 field studies to test their newly developed NEAT method. Their results showed that nanoparticles were emitted during the various processes and occurred in a variety of shapes and sizes, and that the NEAT method proved to be useful in detecting and quantifying nanomaterial emissions. Their research also suggests the capability of immediately measuring emission control effectiveness, such as exhaust ventilation systems (Methner, et al., 2010).

## Direct Reading Instruments

The NIOSH NEAT method calls for the side-by-side use of an OPC and a CPC, as well as filter-based air sampling for airborne mass and electron microscope analyses. A third DRI that may prove to be useful in characterizing particulate matter

aerosolization from the fabrication of ACM panels is a surface area monitor. Particulate surface area is a key parameter discussed earlier and proposed by Maynard as a useful measurement in characterizing aerosol particulates (Maynard & Kuempel, 2005). The three DRIs are further discussed in the following paragraphs.

### *Condensation Particle Counter*

A condensation particle counter (CPC) continuously draws in an aerosol sample at a set flow rate, utilizing a built-in pump. CPCs are generally utilized for detecting particulate matter with diameters of less than 1.0 µm. Immediately after the particles enter into the CPC, they pass through a saturator tube, where they mix with an alcohol solution, usually of at least 99.5 % high purity isopropyl alcohol. From the saturator tube, the particle-alcohol mixture flows into a condenser region, where the alcohol condenses onto the particles in a controlled manner. Thus the particles "grow" into larger droplets of equal size, regardless of their original size (TSI, 2006).

The enlarged particles pass through an optical detector, which is a laser beam that causes a flash of light to be reflected onto a photo-detector. Each flash of light represents a single particle to be counted. A limitation is that if a particle is not able to be grown to the desired size in this process, it will not produce the desired flash of light and miss the opportunity to be detected or counted. Furthermore, because the instrument grows the particles to the same size, it does not differentiate between sizes. The researcher would simply note the number of particles in the aerosol that are less than 1.0 µm, or whatever the maximum particle size of the CPC.

The instrument used in this graphite-epoxy material study is an ultrafine particle counter (UPC), TSI P-Trak 8525, which operates on the same theory as the CPC, but it detects particles with diameters less than 1.0 µm (TSI, 2006) (Hinds, 1999). The P-Trak 8525 detects particles in the size range of 0.01 µm to 1.0 µm and a concentration range of 0-500,000 particles per cubic centimeter (p/cc), having a continuous flow sampling flow rate of about 700 $cm^3$/min (TSI, 2007). However, Ferreri found out from TSI that the P-Trak 8525 has a limit of linearity of 100,000 p/cc (Ferreri, 2010).

### *Optical Particle Counter*

Similar to the CPC, the optical particle counter (OPC) draws in a volume of aerosol via an internally flow-controlled pump. However, instead of growing the particle to a specific size, the particles enter the OPC and immediately pass through a light beam (generally a laser diode) for counting and size measurements. The scattered light is directed, utilizing a mirror, onto a detector that is positioned optically at an angle of incidence to the laser beam, enhancing the capability of collecting the scattered light. The detector organizes the particles into various size bins, as a result of the amount of energy of the light pulse created from passing the laser beam; recall that the CPC lacked this capability.

A limitation of the OPC is that particles may agglomerate and be considered as a larger particle to be misplaced in another sizing bin. There is also the possibility of particles being overshadowed by larger particles during high particle concentration flows. Thus, there are interferences, coincidence losses and counting inefficiencies associated with the optical particle counter. The OPC is highly influenced by the particle's

refractive index and non-spherical shape. The occupational health technician must be aware of these and understand that the OPC is not 100% accurate. The OPC used in this thesis is the GRIMM Portable Aerosol Spectrometer (PAS) 1.108 (S/N 8F100007), which contains 15 size channels and a published reproducibility of ±3%, having an upper particle concentration range of $2.0x10^6$ particles/liter (Hinds, 1999) (GRIMM Aerosol Technik GmbH & Co., 2009).

### *Surface Area Monitor*

The surface area monitor is generally used for nano-sized particles, since their surface area is greater than larger particles of the same mass. Surface area proves to be a useful measurement of dose for ultrafine particles that have the potential to reach the alveolar region of the lung. In his thesis, Ferreri explains the theory behind the surface area measurements utilizing an Electrical Aerosol Detector (EAD), also demonstrated by Wilson *et al* (Wilson, et al., 2007) (Ferreri, 2010). The results of the surface area measurements may be displayed in a size distribution plot, in a similar manner as the particle count distribution from the OPC and CPC data. Unfortunately, the surface area monitor had malfunctioned, so the particle surface area measurements could not be obtained for this thesis research.

# III. Method

For the first part of this research, the author traveled to Hill AFB, UT in order to gather aerosol data on the fabrication of B-2 graphite-epoxy panels. The week-long endeavor began with meeting shop personnel and understanding the operations to be performed on the first day, preparing the equipment on the second day, conducting two days of rigorous sampling, and shipping samples and equipment on the final day.

Large 12-ply panels were cut with a Zimmermann FZ32 CNC 5-axis portal milling machine (Figure 1), designed for automotive and aircraft fabrication, specifically for aluminum and composite materials (F. Zimmermann GmbH, 2007). Parts needed to be cut from three relatively large composite panels. Two pieces of each part will be combined to form a complete 24-ply graphite-epoxy part to be used on the aircraft. The first panel to be cut is shown in Figure 1.


**Figure 1 Zimmermann FZ32 Portal Milling Machine**

Notice in Figure 1 that the FZ32 has an attached local exhaust ventilation (LEV) system, which was functioning at a decreased efficiency due to a broken slider mechanism that would not allow the head of the LEV to lower down to the tip of the cutting bit, where the aerosol would be at the highest concentration. In an attempt to determine the adequacy of this engineering control, aerosol samples were collected with the LEV on and with it off. Face velocity and capture velocity measurements were taken on the LEV before sampling began, demonstrated in Figure 2.

**Figure 2 Measuring face velocity of FZ32's LEV**

Figure 3 displays the four airflow sampling locations for the FZ32 LEV, utilizing an Alnor Compuflow 8570, S/N 02057126, calibrated on 4 June 2010.

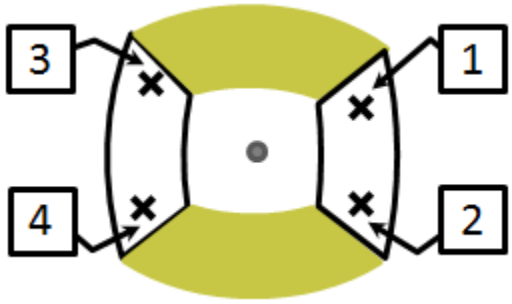


**Figure 3 LEV airflow sampling locations for FZ32**

The four face velocity measurements were averaged, and the average airflow was calculated by multiplying the face velocity by the combination of the two slot areas. There are two slot areas of equal length and diameter, six inches and ½ inch, respectively; therefore, the total area is roughly six square inches, or 0.042 square feet. Table 1 displays the LEV measurements.

**Table 1 FZ32 LEV airflow measurements**

| Location | Vel (fpm) |
|---|---|
| 1 | 5000 |
| 2 | 600 |
| 3 | 6000 |
| 4 | 600 |
| **AVE** | 3050 |
| **Area ($ft^2$)** | 0.042 |
| **Q (cfm)** | 128.1 |

Because the LEV head was stuck in the up position, the capture velocity cannot be maximized by moving the head down closer to the cutting operation. The capture velocity was measured to be 65 fpm at a distance of six to seven inches.

As suggested by Methner, filter-based media sampling was conducted alongside of the direct reading instruments, summarized in Table 2.

**Table 2 Filter media used in B-2 ACM aerosol sampling**

| Filter Size/Type | Purpose | Method |
|---|---|---|
| SKC 37mm, 5µm, PVC | PNOR, Respirable | NMAM 0600 |
| SKC 37mm, 5µm, PVC | PNOR, Total | NMAM 0500 |
| SKC 37mm, 3-piece quartz | Elemental Carbon | NMAM 5040 |
| SKC 47mm PTFE | GRIMM filter | SEM analysis |
| SKC 37mm, 0.8µm, MCE matched wt | Fibers, not asbestos | NMAM 7400 |

The filter media was pre-weighed, having carefully disassembled the cassette to extract the filter, using the local Science and Technology lab on Hill AFB with a Mettler Toledo XP 204 balance (S/N 1129231776). See Appendix A for the summary table of before and after filter weights. One must use extreme caution when performing this task after the particulate matter is collected, as not to lose any of the sample during the disassembly process. It is noteworthy to mention that the balance was only a 4-digit scale, but is representative of what most base-level BEEs will have access to if desiring to perform their own gravimetric analysis. However, the analysis shows that a 6-digit scale is necessary in order to meet the limit of quantification requirements.

Initially, the apparatus was set up as close as possible at the point of operation. It was placed next to the panel, leaving room for the FZ32 to move about, as shown in Figure 4. The FZ32 makes multiple passes along the line of cut, taking off 1/8 inch depth of material at a time until completely cut through.

**Figure 4 Initial setup of the aerosol sampling apparatus**

Figure 5 is a close-up of the aerosol sampling apparatus, as to display the orientation of the sampling media and the intake ports of the direct reading instruments.

**Figure 5 Close-up of the aerosol sampling apparatus**

The operator first used a cubic boron nitride (CBN) bit to cut the 12-ply graphite-epoxy panel, pictured in Figure 6.

**Figure 6 Cubic boron nitride bit in FZ32 core mill**

Figure 7 shows the CBN bit routing through the panel. Notice the large agglomerated particulates on the panel and floor.

**Figure 7 Cutting ACM panel with CBN bit**

Shortly after the photo in Figure 8 was taken, the CBN bit began to overheat and burn the particulate matter as it cut the panel, causing fumes and smoke. Therefore, in order to alleviate the burning of the material, the operator changed the CBN bit to a polycrystalline diamond (PCD) bit, pictured in Figure 8.

**Figure 8 Polycrystalline diamond bit used for majority of ACM panel cutting**

The PCD bit worked better than the CBN bit and was used for the duration of the panel cutting although occasionally the operator had to clean out the grooves with a tool and HEPA vacuum to prevent burning of the particulates. Figure 9 illustrates the FZ32 in action with the PCD bit. One can also see the cloud of aerosol just behind the bit that is moving toward the LEV.

**Figure 9 FZ32 cutting graphite-epoxy panel, showing cloud of particulates**

## CPC Setup

The CPC (blue instrument with a handle) is a TSI P-Trak ultrafine particle counter (model 8525, S/N 12001004). The P-Trak was zeroed just prior to the sampling event with the supplied HEPA zero filter. The intake tube of the CPC is stretched across the top of the OPC, near its short rigid intake tube, as seen in Figure 5. Display units are in particles per cubic centimeter (p/cc), which are converted to particles per liter (p/l) in the analysis to match the units of the OPC. The P-Trak samples continuously, at a nominal flow rate of 0.7 l/min, and records the particle concentration every second, which can be exported into *Microsoft Excel*® (Microsoft, Redmond, WA) for analysis (TSI, 2007).

## OPC Setup

The OPC is a portable aerosol spectrometer (PAS, model 1.108, S/N 8F100007) made by GRIMM Technologies, Inc. (Douglasville, GA) that contains the following 15 output size channels (units in µm): 0.23, 0.30, 0.40, 0.50, 0.65, 0.8, 1.0, 1.6, 2.0, 3.0, 4.0, 5.0, 7.5, 10.0, 15.0, 20.0. The PAS's airflow is internally controlled and set to 1.2 l/min. It has the option of setting the display units in mass ($\mu g/m^3$) or particle concentration (p/l). In order to compare against the CPC, the PAS was set to particle concentration, and the time averaging was set to 1 minute. The aerosol spectrometer's software, version 8.60E, records the raw data of particle number concentrations in the appropriate bucket sizes with corresponding date and time stamp for each data point, which is exported into *Microsoft Excel*® for analysis (GRIMM Aerosol Technik GmbH & Co., 2009).

The PAS requires a 47-mm PTFE filter that is placed on the back side of the instrument, which collects the particulate matter before the air stream exits. The filters were pre-weighed utilizing the same scale at the local Science and Technology lab on Hill AFB. Two filters were actually used, one for each day of sampling, and post-weighed with the same scale. The filters were used for two separate analyses. First, they were analyzed for mass concentration of particulate matter flowing through the PAS, which was compared to the theoretically calculated mass concentration based on the density of the particles (1.75 $g/cm^3$ for carbon fiber) using Hinds equations (Hinds, 1999). See the Analysis section for the equations used. Secondly, the filters were examined for fibers with an SEM at AFIT.

### *GRIMM's PAS Filter Preparation for SEM Analysis*

The 47-mm filter would not fit on the much smaller sample head of the SEM sample holder, also called the stage. Therefore, a portion of the filter was cut, assuming that it would be representative of the homogeneously-assumed whole filter, and weighed with a microbalance to determine what percentage of the filter was being analyzed. Once the sample was placed in the scanning electron microscope (SEM) and the door closed, helium was sent through the SEM to flush out all of the air (oxygen and nitrogen) to decrease the possibility of the sample decomposing under vacuum. A varying pressure aperture was used in the SEM.

## Conventional Filter-Based Air Sampling

Four air sampling pumps from two different manufacturers, Apex Lite and TSI SP730, were calibrated before and after the sampling with an average of 10 cycles with a BIOS Dry Cal DC-Lite (S/N DC-L 2068). Recall the equipment setup in Figure 5. A TSI SP730 (S/N 7300634013) was used for respirable particulate matter (NIOSH Analytical Method 0600) with an aluminum cyclone attached to a 37-mm PVC filter and set at a flow rate of 2.5 L/min for the 4-µm 50% cut-point. Actual calibration was 2.499 l/min. A TSI SP730 (S/N 7300634003) was used for total particulate matter (NIOSH Analytical Method 0500) with a 37-mm PVC filter and set at a flow rate of 2.0 L/min. Actual calibration was 2.003 l/min. The third pump was an Apex Lite (S/N 3991604), having the 37-mm quartz filter for elemental carbon (NIOSH Analytical Method 5040), which was set to 4.0 l/min, according to the method, and calibrated at 3.996 l/min. The

fourth pump, a TSI SP730 (S/N 7300634002), had the 37-mm matched weight MCE filter attached and calibrated to 2.018 l/min, which would be sent to the lab for fiber count (NIOSH Analytical Method 7400) similar to the asbestos method utilizing phase contrast microscopy.

## Analysis

The particle size differentiation in the OPC allows for the creation of a size distribution that can be used to calculate the aerosol mass, comparing it to conventional gravimetric analysis of filter-based air sampling (GRIMM Aerosol Technik GmbH & Co., 2009) (Hinds, 1999). The particle number concentrations exported from the PAS into the spreadsheet were averaged over each of nine sampling time periods that covered the two days, six samples on the first day and three sample periods on the second day. The mass median diameter (MMD), used as a mathematical expression of particle size, of the averaged aerosol data was calculated using Equation 1 (Hinds, 1999).

$$d_{mm} = \left(\frac{m_1}{M} d_1 + \frac{m_2}{M} d_2 + \cdots + \frac{m_I}{M} d_I\right) \quad (1)$$

where

$d_{mm}$ = *mass median diameter* (μm)

$m$ = *mass concentration* (mg/m$^3$), calculated as $C_m$ in Equation 3

$M$ = *sum of individual mass concentrations* (mg/m$^3$)

$d$ = *average diameter of the bin size range* (μm)

According to Hinds, the count median diameter (CMD) is also known as the geometric mean for log-normal data, which is generally the case for aerosol sampling data, and is calculated by Equation 2 (Hinds, 1999).

$$CMD = d_g = e^{(\frac{\Sigma n_i \ln d_i}{N})} \quad (2)$$

where

$d_g$ = *count median diameter* (µm)

$n$ = *number of particles in particular bin*

$d$ = *average diameter of the bin size range* (µm)

$N$ = *total number of particles in all the bins*

The mass concentration of particles is calculated using Equation 3 (Hinds, 1999). The density of the particle must be known for this equation.

$$C_m = C_n(\rho\frac{\pi}{6})(D_m)^3 \quad (3)$$

where

$C_m$ = *mass concentration* (mg/m$^3$)

$C_n$ = *number of particles in particular bin*

$D_m$ = *diameter of average mass* (µm)

The diameter of the average mass, $D_m$, is calculated by summing the quotients of each bin diameter cubed divided by the cubed root of each average particle count in the particular bin. In mathematical form, $D_m = \Sigma((\text{Bin Diameter})^3/\text{Avg Part Count})^{1/3})$.

Realizing that the particle size range for the CPC is 0.02 µm to 1.0 µm, and the range for the PAS is 0.3 µm to 20 µm, a technique must be created in order to combine the two sets of data, unless it is desired to present them as a comparison. Several studies have been performed that combine OPC and CPC data, including the count-difference method by Schmoll *et al*. and a technique of creating a new bucket size range from the CPC data to be combined with the buckets of the OPC, by Heitbrink *et al*., which Ferreri used in his thesis (Heitbrink, et al., 2009) (Schmoll, Peters, & O'Shaughnessy, 2010) (Ferreri, 2010). For this research, the approach utilized by Heitbrink *et al*. was used. Therefore, the equation used to create the new bucket size range of 0.02 µm to 0.30 µm from the CPC data is shown in Equation 4.

$$C_{0.020-0.300\ \mu m} = N_{cpc} - \sum_{i=1}^{5} C_{n,i} \tag{4}$$

where

$C_{0.020\text{-}0.300\ \mu m}$ = *number of particles in the new size bin*

$N_{cpc}$ = *average number of particles obtained by the CPC*

$C_{n,i}$ = *number of particles in* $i^{th}$ *OPC bin*

Notice the particle concentrations are being summed from buckets 1 to 5, because the upper limit of the 5$^{th}$ bucket of the PAS happens to be the maximum size range of the

CPC (i.e. 1 µm). Utilizing Equations 1-4, the mass median diameter (MMD), count median diameter (CMD), and mass concentration of the particles ($C_m$) were calculated, combining the data from the PAS and CPC. Combining the CPC and OPC data allowed for the creation of a complete particle size distribution from 0.02 µm to 20 µm, although it was only needed to go up to 4 µm for modeling deep lung and up to 10 µm for modeling total respiratory exposure potential.

## C-17 Crash Methodology and Analysis

Aerosol sampling for the C-17 crash was conducted on the demolition of a portion of burned tail section consisting mostly of ACM. Although very unfortunate, this aircraft mishap at Elmendorf AFB, which happened on 28 July 2010, served as a follow-up research to Capt Ferreri's burned ACM ticket bench top experiment. The United States Air Force School of Aerospace Medicine (USAFSAM) assisted in gathering the data. It is significant to mention that it was raining, and it had been raining for 32 days straight. This is a good situation for the crew that had to clean up the debris. However, it made it difficult to collect the needed data for comparison.

A chop saw, similar to a concrete saw used in construction, was the tool of choice for crash recovery workers who cut a large portion of the tail section. An excavator with a clamshell was also used to crush some of the debris into smaller sections in order to place in boxes. Crew members walked about the hot zone picking up smaller pieces, separating out the ACM from other materials. A solution of water and wax was sprayed on any part that appeared to be advanced composite material using backpack type

sprayers similar to herbicide and pesticide sprayers, which was in addition to the debris being rain-soaked.

The direct reading instruments (DRIs) that were used in the C-17 crash aerosol sampling are as follows: CPC, TSI 3007 (S/N 07080003) and OPC, GRIMM PAS 1.108 (8F100007). The author could not stay in the hot zone for the duration of the sampling. For each sampling period, the instruments were taken into the hot zone, where they were set up, turned on, and retrieved at shift change. The DRIs were placed on a tripod downwind from the demolition of the tail section, at a distance of approximately 50 meters, in order to protect the instruments. However, they were located in a reasonable position as to obtain data representative of that to which crash recovery members might be exposed. It is acknowledged that the diesel exhaust from the excavator and concrete saw may cause interference with aerosol collection of the ACM particles. The crew wore a complete personal protective equipment ensemble of Tyvek® coveralls, nitrile gloves, rubber boots, and full-face air purifying respirator with organic vapor cartridges.

For the purpose of this thesis, the only data to be analyzed is that of the CPC and OPC used during the aerosol sampling of the downed C-17 demolition of the vertical and horizontal stabilizers, in the same manner as that of the B-2 sampling data analysis. Gravimetric analysis, NMAM 5040 and NMAM 7400 were not performed. The intent is to show that the CPC and OPC can be utilized out in the field, whether on newly fabricated ACM panels or for crash and recovery operations on downed aircraft containing ACM.

# IV. Results/Discussion

## Aerosol Sampling of Cutting B-2 Graphite-Epoxy Panel

### *Gravimetric*

Although the instruments would normally be located on the operator to assess worker exposure, they were actually placed near the point of operation. For this thesis and research objectives, evaluation of worker exposure was not accomplished. It is assumed that if the area sampling shows the current engineering controls are working properly, the personnel exposures will subsequently be decreased.

For the gravimetric analysis, a 4-digit scale, rather than the needed 6-digit microbalance, was utilized at the local Science and Technology lab at Hill AFB. Out of 16 filters, only one for total particulate matter (PM) met the required mass for the limit of quantification (LOQ). However, because there was a significant amount of mass on this filter, it increased the average of the seven filters used for total PM, yet still below the LOQ. Since the required LOQ for total PM is 1.528 mg, 1.155 mg for respirable PM, and 1.155 mg for PM on the PAS filters, the gravimetric analysis is invalid. This shows that even though gravimetric analysis is the "gold standard" for determining personnel exposure and health risk, it is not of much use for base-level BEEs when sampling for ultrafine particles.

The average mass collected for total particulate matter (PM) was 1.319 mg, and the average mass collected for respirable particulate matter was 0.317 mg. A summary of the PM gravimetric analysis is displayed in Table 3, and the filter weights are recorded in Appendix A.

**Table 3 Summary of particulate matter gravimetric analysis**

| | Avg Mass (mg) | Avg Std Dev (mg) | LOQ (mg) | Meets LOQ? |
|---|---|---|---|---|
| **Total PM** | 0.9619 | 1.3187 | 1.5275 | No |
| **Respirable PM** | 0.1952 | 0.3171 | 1.1547 | No |
| **GRIMM PAS** | 0.4833 | 0.4478 | 1.1547 | No |

Due to the 4-digit balance used for weighing the filters, the limit of quantification (LOQ) was not met. Table 4 shows the results of the elemental carbon (NMAM 5040) air sampling, which was sent off to a contract laboratory for analysis via a flame-ionization detector, a thermal-optical analysis technique.

**Table 4 NMAM 5040 Elemental Carbon Results**

| Sample No. | Mass (µg)[1] | Conc. (µg/m$^3$)[2] | Comments |
|---|---|---|---|
| 001A | 55 | 0.640 | LEV off |
| 002A | 2.1 | 0.024 | LEV on |
| 003A | 220 | 2.558 | |
| 004A | 730 | 8.488 | Operator cleaning out grooves, overburdened LEV |
| 005A | < 2 | - | Blank 1 |
| 006A | < 2 | - | Blank 2 |
| 1. This is mass of elemental carbon; not blank corrected | | | |
| 2. Proposed ACGIH Standard is 20 µg/m$^3$ (if personnel sampling) | | | |

Six samples were also sent to the contract laboratory to be analyzed using NMAM 7400b (fibers other than asbestos), which calls for the technique of phase contrast microscopy (PCM). Mixed-cellulose ester (MCE) membrane filters are used in NMAM 7400 because they are biologically inert, low in metal background, and dissolve easily when exposed to acetone, leaving only the fibers to be counted under a light microscope. A summary of the results is shown in Table 5.

**Table 5 Fiber analysis results using NMAM 7400b**

| Sample No. | Air Volume (L) | Fiber Conc. (fibers/cc) | Comments |
|---|---|---|---|
| 5860 | 118 | 0.24 | |
| 5880 | 0 | - | Blank |
| 5903 | 0 | - | Blank |
| 5904 | 44 | 0.25 | |
| 5899 | 131 | 0.049 | |
| 5889 | 90 | 0.30 | |
| 1. Filters analyzed by NMAM 7400b, fibers other than asbestos | | | |
| 2. No standard exists for carbon fibers | | | |

The bulk of the analysis and results for this thesis is for the OPC and CPC, demonstrating their importance in field studies for capturing ultrafine particulate matter data. The CPC data is primarily displayed in charts that show the particle concentration peaks. As explained in the Analysis section, a new size bin was created to combine the CPC data with the OPC (GRIMM PAS) data and graphs and tables are utilized to display the results. Figure 10 is a chart of all the CPC data from DAY 1, and DAY 2's data is shown in Figure 11. The three pauses (around 8:18, 8:33-9:02, 9:50) indicate when the operator stopped the FZ32 for adjusting the panels or to place the next panel to be cut on the pedestal.

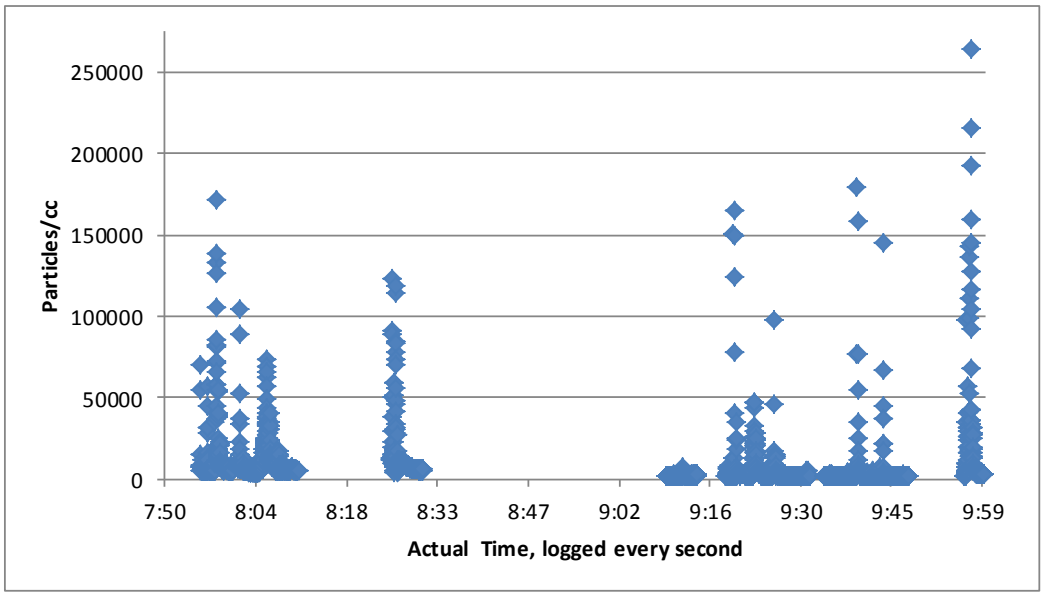


**Figure 10 CPC sampling of cutting graphite-epoxy panels on DAY 1**

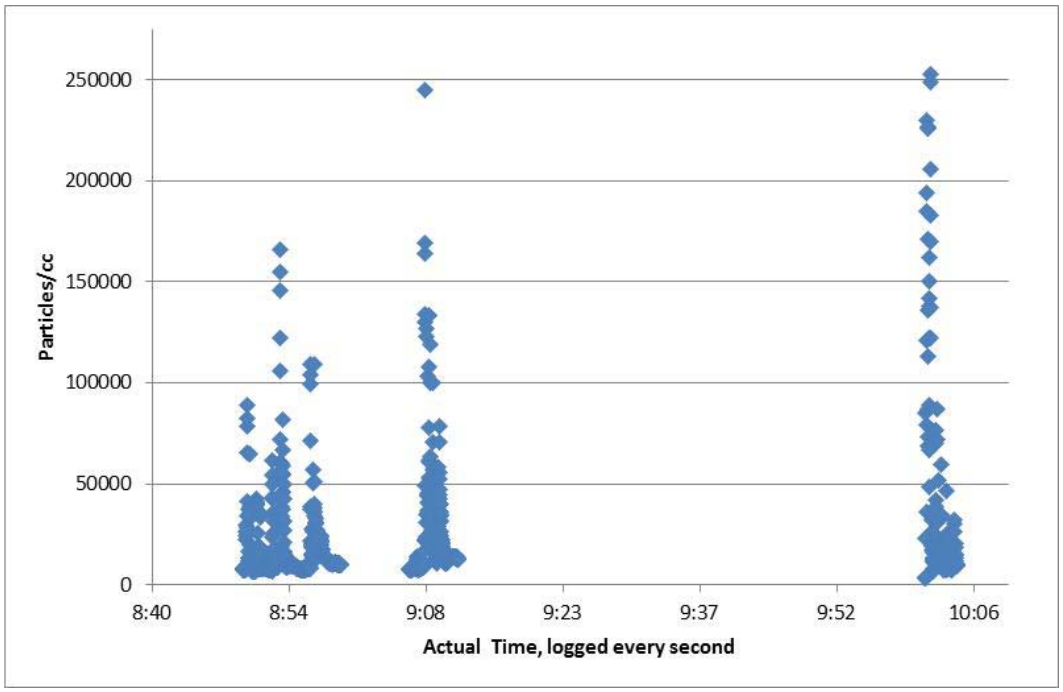


**Figure 11 CPC sampling of cutting graphite-epoxy panels on DAY 2**

In Figures 10 and 11, there were six sampling events on DAY 1 and three on DAY 2. The particle concentration for the first sampling period (Day 1a) is displayed in Figure 12, where the horizontal axis is the actual time of sampling on 23 June 2011, and particles per cubic centimeter is on the vertical axis. The other charts, for the remaining eight sampling periods, are displayed in Appendix B.

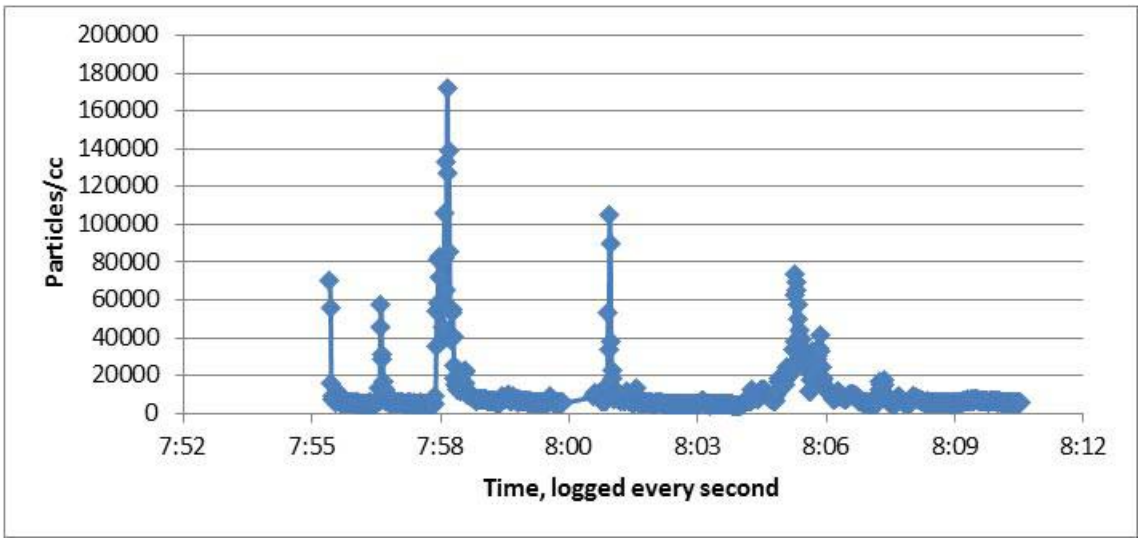


**Figure 12 CPC sampling, first time period of DAY 1**

There were three particular instances (three out of 6085 data points) in which the CPC reached its maximum concentration range of 500,000. The instruments were closely monitored and pulled back as to minimize the number of times that the maximum concentration is reached. Another drawback of the data is that the limit of linearity is 100,000 p/cc and there were 143 out of 6085 data points (2.35% of the data) that exceeded this value. The data are used as an estimation of particle count for creating the distribution curve for the aerosol generated at the point of operation, or as close as possible without interfering with the process. Due to the exceedance of the limit of

linearity, those data points should be used cautiously and not as actual exposure concentration. The particle count is averaged for each sample period when combined with the optical particle counter.

The graphs and table that follow are from the first sampling set on the first day (DAY 1a), which display the results of the combined CPC and OPC data. Figure 13 is a graph of DAY 1a's particle concentration per diameter size channel, and Figure 14 displays the aerosol mass concentration per diameter size channel.

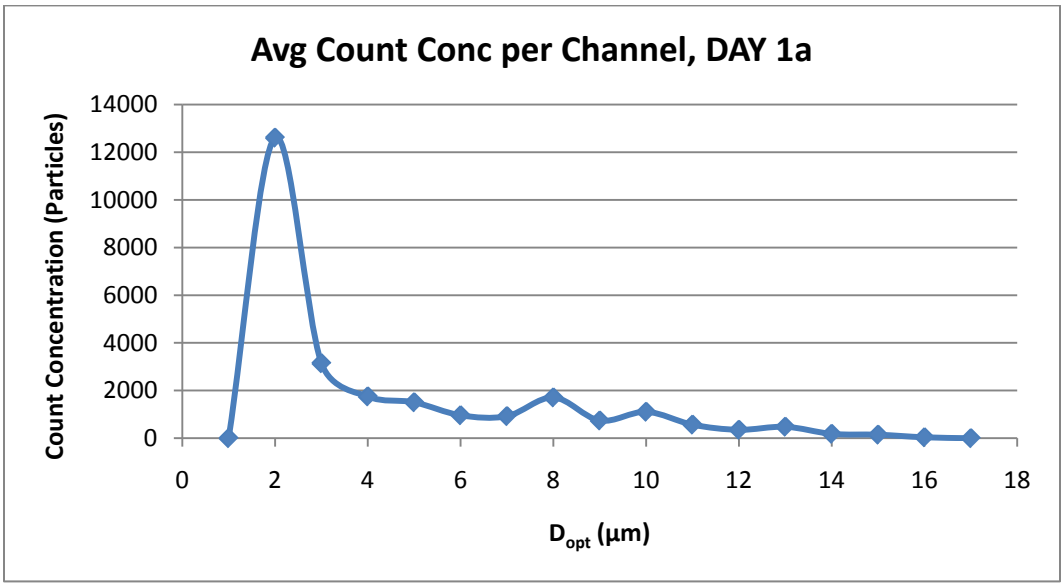


**Figure 13 Combined CPC and OPC particle count size distribution for DAY 1a**

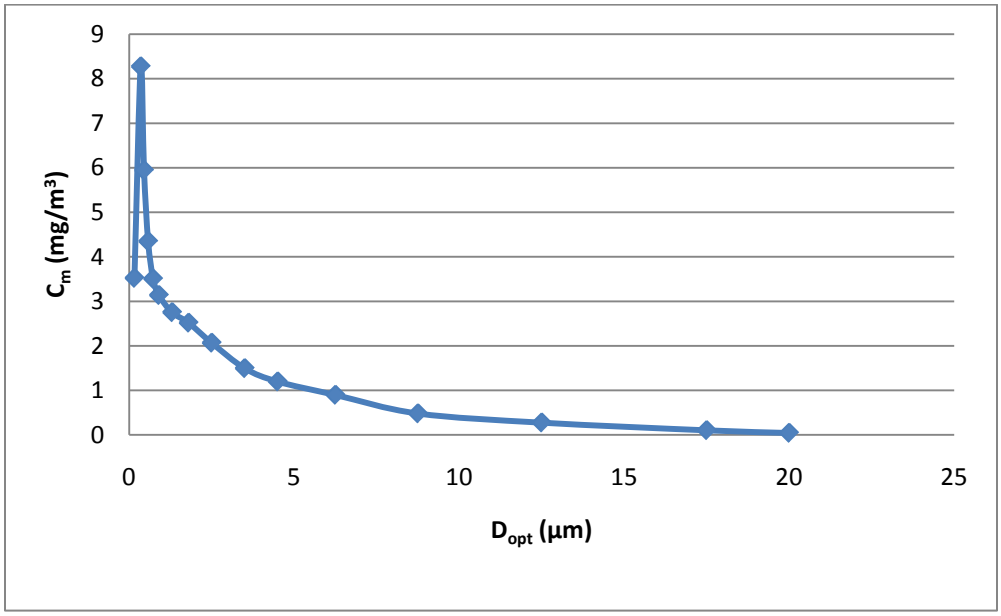


**Figure 14 Combined CPC and OPC particulate mass size distribution for DAY 1a**

The results of the mass median diameter, MMD ($d_{mm}$), CMD ($d_g$) and mass concentration of the aerosol for time period DAY 1a are displayed in Table 6.

**Table 6 Calculated MMD, CMD and mass concentration for DAY 1a**

| | | |
|---|---|---|
| **Mass Median Diameter, $d_{mm}$:** | **6.37** | **µm** |
| **Count Median Diameter, $d_g$:** | **0.74** | **µm** |
| **Mass Concentration:** | **2.5363** | **mg/m$^3$** |
| **GM:** | **1.24** | **µm** |
| **GSD:** | **1.02** | |

Rather than displaying the series of graphs and tables for the remaining eight sets of sampling periods, which are similar to that of DAY 1a, Table 7 presents the calculated MMD, CMD, $C_m$, geometric mean and geometric standard deviation of the nine sets of graphite-epoxy aerosol samples.

**Table 7 Summary of calculated MMD, CMD and mass concentration for the nine samples**

| Sample | MMD, µm | CMD, µm | $C_m$, mg/m$^3$ | GM | GSD |
|---|---|---|---|---|---|
| **Day1a** | 239.0503 | 0.6752 | 136.8942 | 1.43 | 1.02 |
| **Day1b** | 268.3531 | 0.8295 | 128.8437 | 1.23 | 1.01 |
| **Day1c** | 44.8199 | 0.7940 | 21.4206 | 1.26 | 1.02 |
| **Day1d** | 106.5560 | 0.3407 | 170.3774 | 2.19 | 1.01 |
| **Day1e** | 6.3984 | 0.4836 | 15.9223 | 1.83 | 1.01 |
| **Day1f** | 27.4132 | 0.4079 | 63.3718 | 1.46 | 1.01 |
| **Day2a** | 12.0943 | 0.4805 | 39.2193 | 1.14 | 1.01 |
| **Day2b** | 63.5315 | 0.4591 | 129.6584 | 1.25 | 1.01 |
| **Day2c** | 198.6693 | 0.9634 | 99.6953 | 1.33 | 1.03 |
| **Average** | 107.4318 | 0.6038 | 89.4892 | 1.46 | 1.01 |
| **StdDev** | 101.9139 | 0.2179 | 56.2486 | 0.34 | 0.01 |

The average count median diameter of the nine sampling periods for the combined CPC and OPC data is 0.604 µm, with a standard deviation of 0.218 µm. The calculated average mass concentration is 89.49 mg/m$^3$ with a standard deviation of 56.25 mg/m$^3$.

### *Instrument Placement*

The peaks for the single sampling period in Figure 12 illustrate that the FZ32 was making passes back and forth. The instruments were located at one end of the panel,

demonstrating the bulk of the particles fall out or are blown along a different path from the location of the instruments. The variation in particle concentration, as well as unknown transport path, would make it difficult to estimate exposure to the operator, who often must enter the core mill chamber to adjust the panel or clean out the grooves so the cutter may make the next path without overheating.

Figure 4 in the Methodology section showed the initial placement of the sampling apparatus. During the first ten minutes of cutting, it was realized that there was a small draft that flowed from the rear of the booth toward the front doors, which were left open to allow the operator better visual acuity and quick entry if needed. The draft may have been causing the smaller particles to be blown away from the instruments, so the DRIs were moved to a location between the FZ32 and front doors for the second round of sampling (DAY 1b), as shown in Figure 15. However, the particle count data does not clearly show that this helped in capturing more aerosol particulates.

**Figure 15 Moved DRIs between FZ32 and doors**

### *ANOVA on CPC Data*

A single factor one-way ANOVA of the CPC data was performed to analyze the variances between and within the nine sets of sampling periods, where 198 random particle count concentrations were extracted from each data set (based on the smallest data set) and normalized by taking their natural logarithm. The data were normalized after visualizing a log-normal distribution curve in JMP 8.0® (SAS Institute Inc.; Cary, NC), as most aerosol sampling data generally follows a log-normal distribution pattern. The JMP 8.0® outputs for the distribution of the data (complete and divided into sampling periods) are found in Appendix C. The 95% confidence ($\alpha$=0.05) single factor ANOVA of the nine CPC sample periods are presented in Table 8.

**Table 8 Single factor ANOVA on the nine CPC sampling sets**

| Anova: Single Factor | | | | | | |
|---|---|---|---|---|---|---|
| | | | | | | |
| SUMMARY | | | | | | |
| *Groups* | *Count* | *Sum* | *Average* | *Variance* | | |
| 1a | 198 | 1718.174 | 8.6776 | 0.5394 | | |
| 1b | 198 | 1799.153 | 9.0866 | 0.3114 | | |
| 1c | 198 | 1575.824 | 7.9587 | 0.4578 | | |
| 1d | 198 | 2113.495 | 10.6742 | 0.6650 | | |
| 1e | 198 | 1958.05 | 9.8891 | 0.0080 | | |
| 1f | 198 | 1743.034 | 8.8032 | 0.3032 | | |
| 2a | 198 | 1871.075 | 9.4499 | 0.3650 | | |
| 2b | 198 | 1925.368 | 9.7241 | 0.5339 | | |
| 2c | 198 | 1977.032 | 9.9850 | 1.0632 | | |
| | | | | | | |
| | | | | | | |
| ANOVA | | | | | | |
| *Source of Variation* | *SS* | *df* | *MS* | *F* | *P-value* | *F crit* |
| Between Groups | 1059.773 | 8 | 132.4717 | 280.7361 | 0 | 1.9436 |
| Within Groups | 836.6299 | 1773 | 0.4719 | | | |
| | | | | | | |
| Total | 1896.403 | 1781 | | | | |

The single factor ANOVA for the nine CPC sampling sets returned that the F-ratio (281) exceeded the F-critical value (1.94) with a p-value less than 0.0001, therefore rejecting the null hypothesis that all the sampling sets contain roughly equal variances. In other words, at least two of the CPC sampling data sets differ with-respect-to the natural logarithm of the particle concentrations.

Similarly, a single factor one-way ANOVA was performed on the aerosol mass concentrations for the nine sampling periods utilizing the combined OPC and CPC data, which is displayed in Table 9.

**Table 9 ANOVA on aerosol mass concentration for combined OPC and CPC data**

Anova: Single Factor

SUMMARY

| *Groups* | *Count* | *Sum* | *Average* | *Variance* |
|---|---|---|---|---|
| 1a | 16 | 2190.308 | 136.8942 | 19384.97 |
| 1b | 16 | 2061.5 | 128.8437 | 11065 |
| 1c | 16 | 342.7295 | 21.42059 | 302.5233 |
| 1d | 16 | 2726.038 | 170.3774 | 176088.1 |
| 1e | 16 | 254.7576 | 15.92235 | 1033.489 |
| 1f | 16 | 1013.949 | 63.37179 | 13552.76 |
| 2a | 16 | 627.5095 | 39.21934 | 6054.491 |
| 2b | 16 | 2074.535 | 129.6584 | 65306.35 |
| 2c | 16 | 1595.124 | 99.69528 | 6841.396 |

ANOVA

| *Source of Variation* | *SS* | *df* | *MS* | *F* | *P-value* | *F crit* |
|---|---|---|---|---|---|---|
| Between Groups | 404979.9 | 8 | 50622.49 | 1.520555 | 0.155601 | 2.007635 |
| Within Groups | 4494437 | 135 | 33292.12 | | | |
| | | | | | | |
| Total | 4899416 | 143 | | | | |

The single factor ANOVA for the combined OPC and CPC sampling sets returned that the F-ratio (1.52) is less than the F-critical value (2.01) with a p-value of 0.156. Therefore, the null hypothesis that all the sampling sets contain roughly equal variances cannot be rejected. In other words, at least two of the samples for the combined data have similar variances with-respect-to the natural logarithm of the particle concentrations, resulting in an insignificant difference between samples.

An alternate way of performing an ANOVA on the CPC data in JMP 8.0® was to insert the normalized particle counts into one column and whether or not the LEV was

turned on or off in the second column. The output of the ANOVA is displayed in Figure 16 and Table 10.

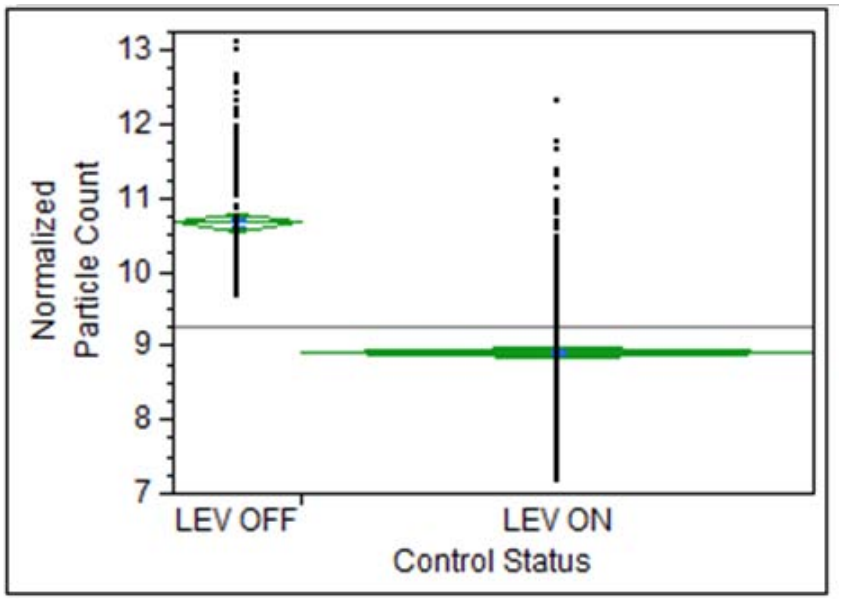


**Figure 16 JMP® ANOVA for CPC normalized particle count vs. control status**

**Table 10 JMP ANOVA table for CPC normalized particle count**

| Source | DF | Sum of Squares | Mean Square | F Ratio | Prob > F |
|---|---|---|---|---|---|
| Control Status | 1 | 496.9151 | 496.915 | 632.4939 | <.0001* |
| Error | 988 | 776.2164 | 0.786 | | |
| C. Total | 989 | 1273.1315 | | | |

The p-value is less than 0.0001 (with a 95% confidence), indicating a significant difference between particle counts with the local exhaust ventilation on and the particle counts with the LEV turned off. In other words, the ANOVA concludes that the particle counts are higher for LEV on versus LEV off. Although the LEV was not operating as

designed, able to move down the bit just above the panel, it was still performing better than if it was turned off.

***SEM***

The scanning electron microscope (SEM) used in this research is a Zeiss EVO® LS 10, which is marketed for materials analysis. A polytetrafluoroethylene (PTFE) control filter (SKC 225-2748), which is utilized in the GRIMM PAS, was used to set up the parameters for the SEM in preparation for the aerosol sample filters. The condition parameters for the control filter are displayed in Table 11.

**Table 11 SEM conditions for PTFE control filter**

| Parameter | Setting |
|---|---|
| EHT | 25.0 kV |
| Working Distance | 7.0 mm |
| Filament Current | 2.606 A |
| Beam Current | 80 µA |
| Aperture | Variable Pressure |

A portion of the PTFE control filter is shown in Figure 17, which is an exported photo from the SEM. For reference, notice the particulate matter in the "blank" control.

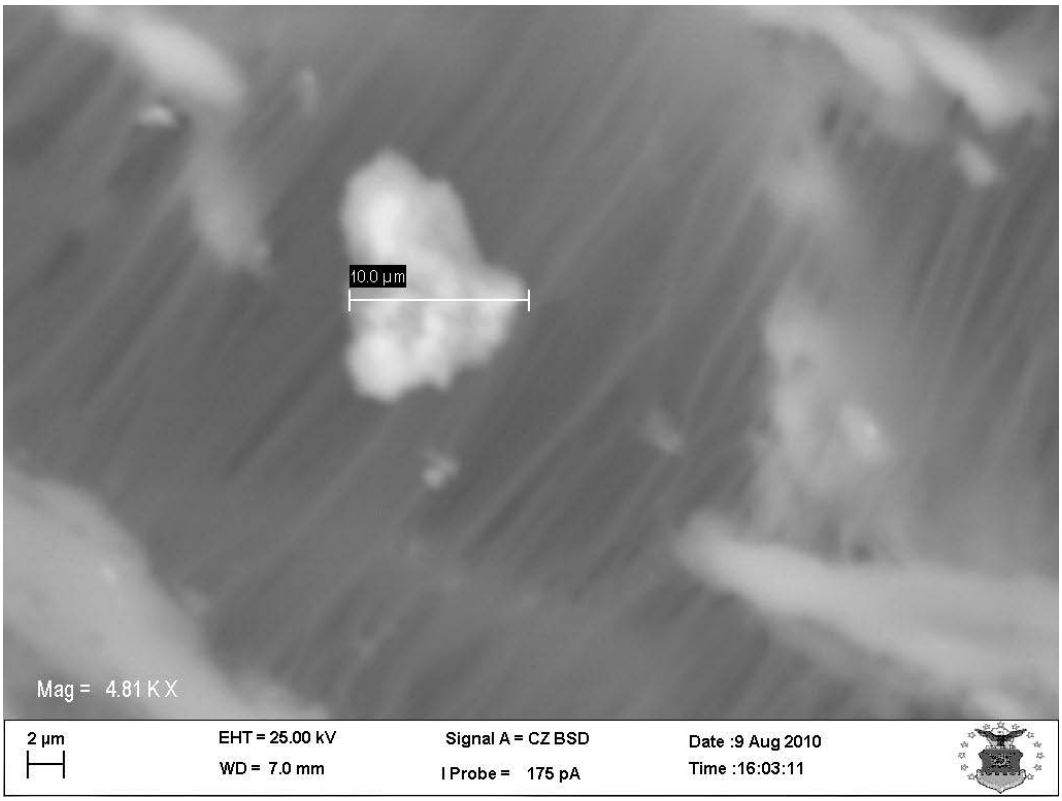


**Figure 17 PTFE control filter for PAS, with particulate matter**

Figure 18 is an SEM image of a portion of PTFE filter that was in the GRIMM PAS during aerosol sampling of the B-2 graphite-epoxy panel cutting operation, showing a potential carbon fiber. Figure 19 is an SEM image of the same fiber, but zoomed in to visualize the fiber's diameter.

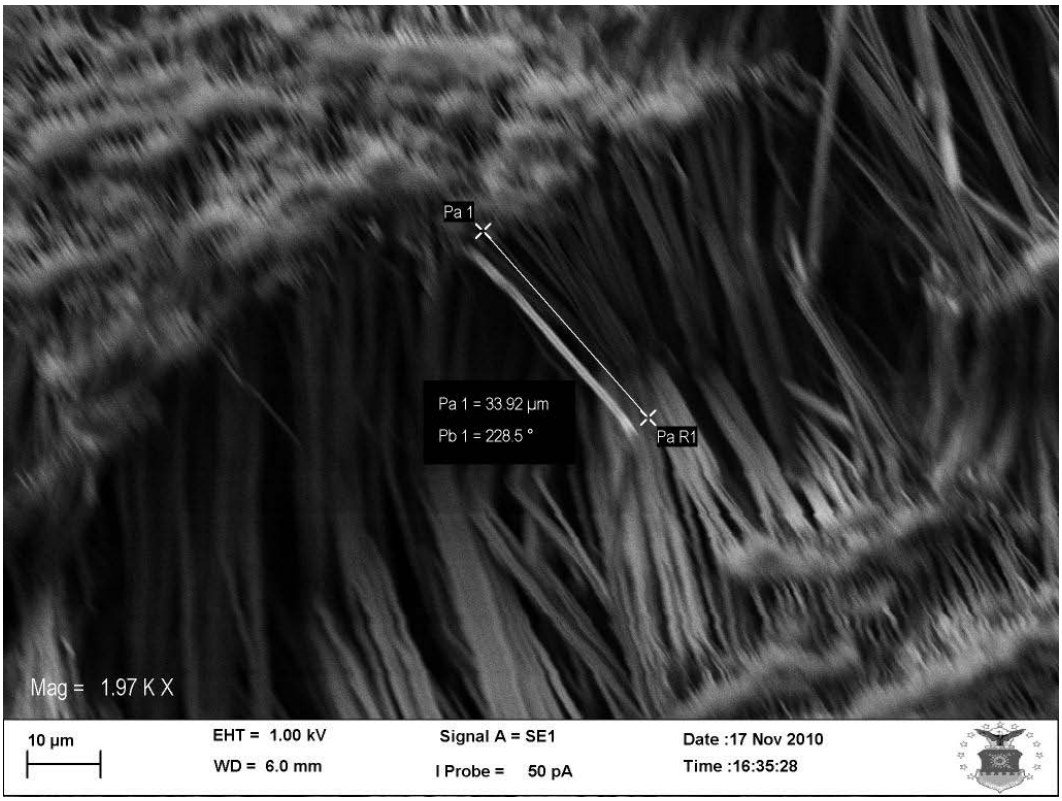


**Figure 18 Potential graphite fiber trapped in the PTFE filter**

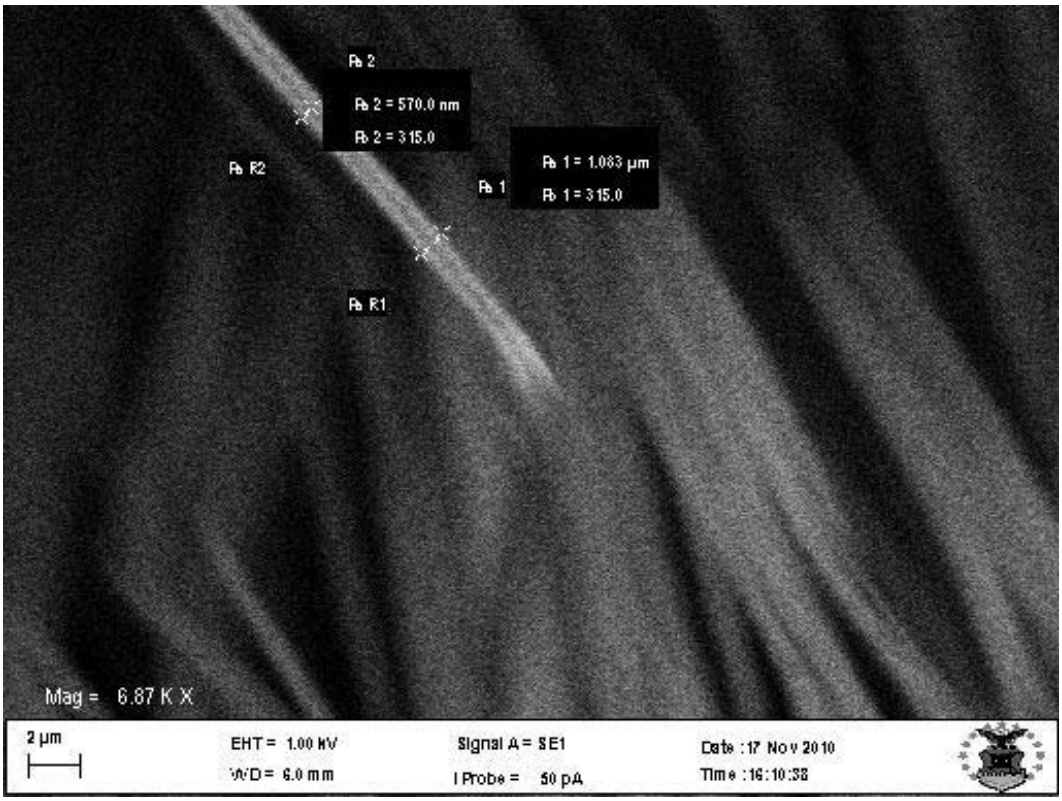


**Figure 19 Zoomed in image of Figure 18, PTFE filter used in PAS**

The SEM condition parameters for the above filter used in the B-2 graphite-epoxy are shown in Table 12.

**Table 12 SEM condition parameters for GRIMM PAS filter used in B-2 sampling**

| Parameter | Setting |
|---|---|
| EHT | 1.0 kV |
| Working Distance | 6.0 mm |
| Beam Current | 20 pA |
| Pressure | 10 Pa |
| Aperture | 100 µm |

### *SEM Discussion on B-2 Panels*

Referencing the potential fiber of Figures 18 and 19, notice that the fiber is a similar shape as those of the filter paper. There is a high likelihood that this may be a carbon fiber as it has a higher conductivity than the other fibers. An illumination occurs as the carbon fiber begins to decompose under vacuum as the electrons make contact with the sample (Viswanathan, Rooke, & Sherwood, 1997). However, it was the only visible fiber noticed for this portion of the filter. There may have been more fibers, but it is a tedious and lengthy process to cover the entire portion and would have taken an enormous amount of time to analyze the entire filter sample.

## C-17 Crash Aerosol Sampling Results and Discussion

### *CPC Results*

The particle count concentrations of the C-17 crash and recovery operations, recorded by the TSI 3007, are displayed in Figures 20-22. The concentrations are not adjusted for background levels. A limitation to this data is that there may be interference due to the exhaust particulates from the concrete saw, forklifts and excavator. Note that in Figure 20, the CPC had faulted and turned off, collecting data for only a portion of the tail section demolition.

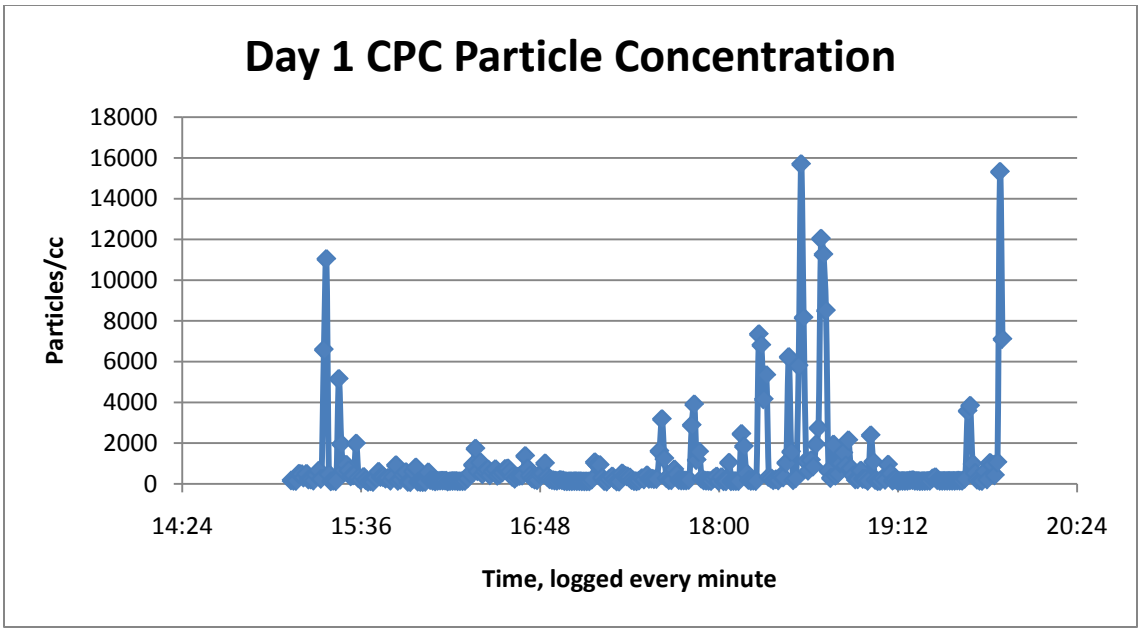


**Figure 20 Results of CPC particle concentration from Day 1 of C-17 crash recovery**

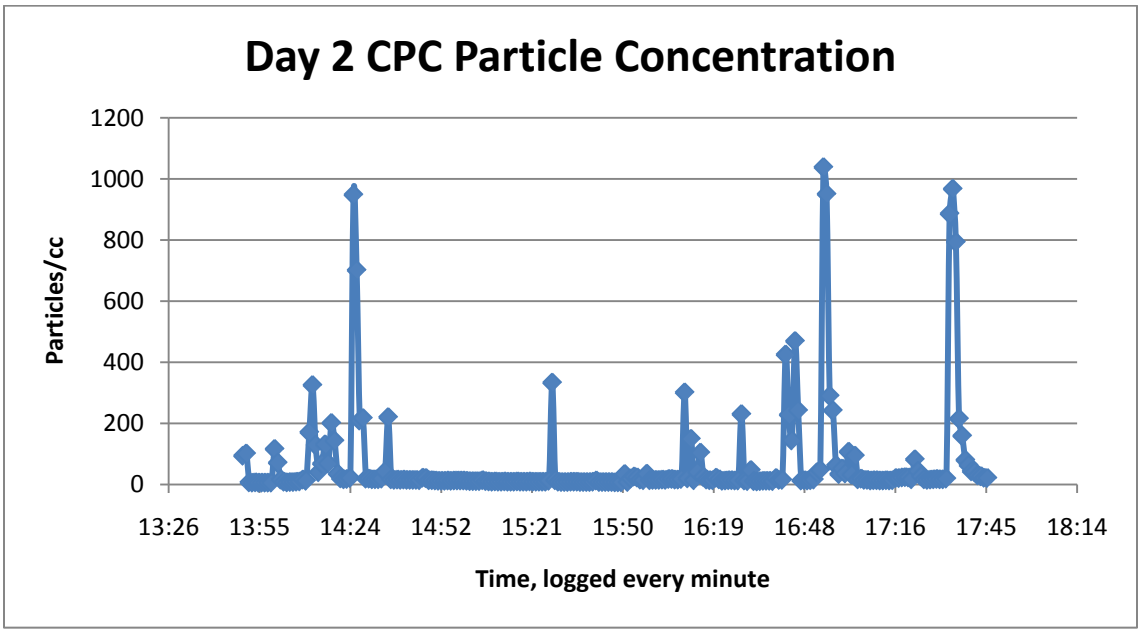


**Figure 21 Results of CPC particle concentration from Day 2 of C-17 crash recovery**

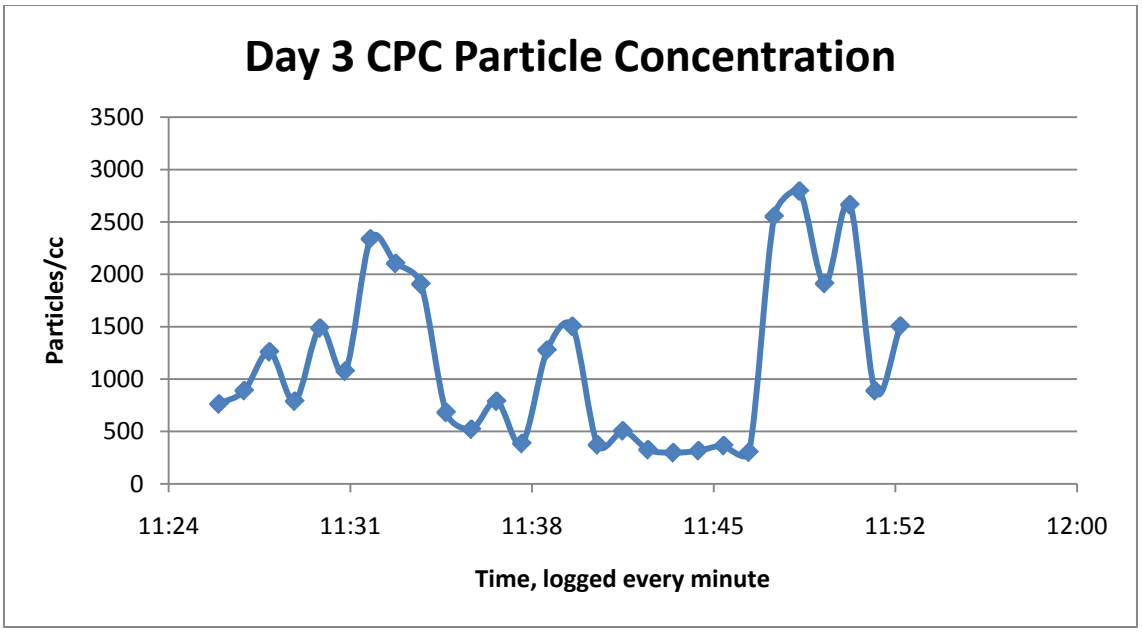


**Figure 22 Results of CPC particle concentration from Day 3 of C-17 crash recovery**

A single factor one-way ANOVA of the CPC data was performed to analyze the variances between and within the three sets of sampling periods, where 28 random particle count concentrations were extracted from each data set (based on the smallest data set of Day 3) and normalized by taking their natural logarithm. The ANOVA results are displayed in Table 12.

**Table 13 Single factor ANOVA on the three CPC sampling sets**

Anova: Single Factor

SUMMARY

| *Groups* | *Count* | *Sum* | *Average* | *Variance* |
|---|---|---|---|---|
| Day 1 | 28 | 161.0721 | 5.752574 | 1.290971 |
| Day 2 | 28 | 88.31702 | 3.154179 | 1.493931 |
| Day 3 | 28 | 190.6781 | 6.809933 | 0.555347 |

ANOVA

| *Source of* | *SS* | *df* | *MS* | *F* | *P-value* | *F crit* |
|---|---|---|---|---|---|---|

| *Variation* | | | | | | |
|---|---|---|---|---|---|---|
| Between Groups | 198.1859 | 2 | 99.09294 | 88.999 | 3.59E-21 | 3.109311 |
| Within Groups | 90.18672 | 81 | 1.113416 | | | |
| Total | 288.3726 | 83 | | | | |

The ANOVA results show an F-ratio of 89.0, which exceeds the tabulated value of 3.1 (F-critical), and a p-value that is essentially zero. Therefore, since the F-ratio exceeds the tabulated F-critical value at the 0.05 level of confidence, the null hypothesis of equal variances among sampling sets is rejected. This means that at least two of the sampling sets have significantly different variances.

### *OPC, GRIMM PAS Results*

In the same manner as the B-2 sampling, an additional bucket size of 0.02-0.3 µm was created in order to combine the CPC and OPC data. The graphical representation of the particle count and mass concentrations per size channel for the first day of sampling are displayed in Figure 23.

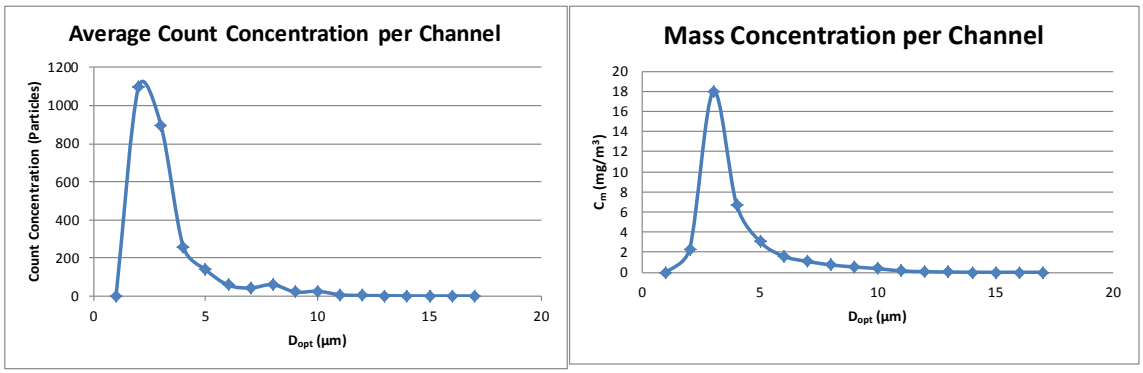


**Figure 23 Combined CPC and OPC particle count and mass concentration per size bin for Day 1**

The results of the mass median diameter, MMD, CMD and mass concentration of the aerosol for the first day of sampling, Day 1, are displayed in Table 14.

**Table 14 Calculated MMD, CMD and mass concentration for Day 1**

| | | |
|---|---|---|
| **Mass median diameter, $d_{mm}$:** | **1.3927** | **µm** |
| **Count median diameter, $d_g$:** | **0.4362** | **µm** |
| **Mass concentration:** | **2.2203** | **mg/m$^3$** |
| **GM:** | **1.2077** | **µm** |
| **GSD:** | **1.0013** | |

Figures 24-25 and Tables 15-16 display the results for the combined CPC and OPC data for the second and third days of aerosol sampling for the C-17 crash and recovery operation.

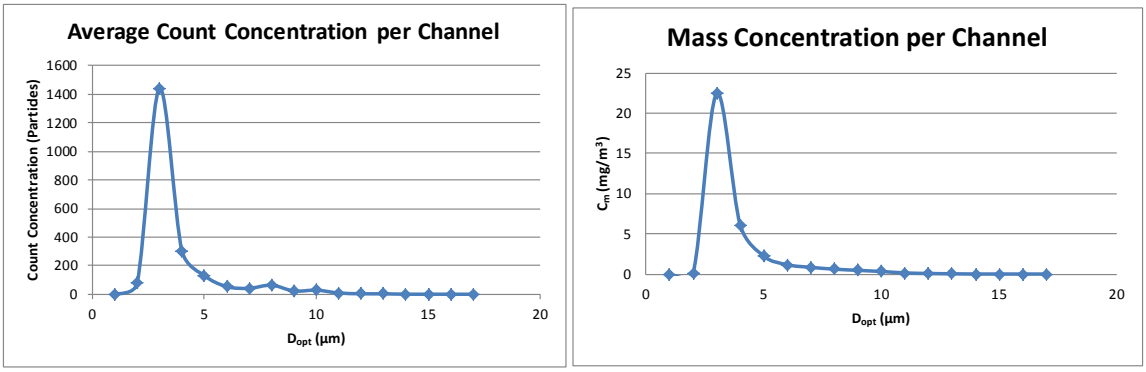


**Figure 24 Combined CPC and OPC particle count and mass concentration per size bin for Day 2**

**Table 15 Calculated MMD, CMD and mass concentration for Day 2**

| | | |
|---|---|---|
| **Mass median diameter, $d_{mm}$:** | **1.0047** | **µm** |
| **Count median diameter, $d_g$:** | **0.4289** | **µm** |
| **Mass concentration:** | **1.4616** | **mg/m$^3$** |
| **GM:** | **1.1307** | **µm** |
| **GSD:** | **1.0010** | |

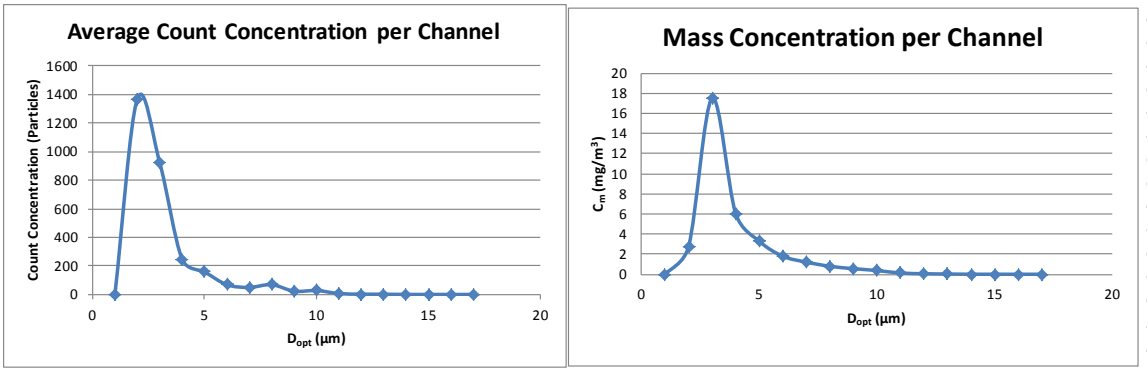


**Figure 25 Combined CPC and OPC particle count and mass concentration per size bin for Day 3**

**Table 16 Calculated MMD, CMD and mass concentration for Day 3**

| | | |
|---|---|---|
| **Mass median diameter, $d_{mm}$:** | **1.0986** | **µm** |
| **Count median diameter, $d_g$:** | **0.4595** | **µm** |
| **Mass concentration:** | **1.4489** | **mg/m$^3$** |
| **GM:** | **1.2238** | **µm** |
| **GSD:** | **1.0014** | |

The average CMD for the three days is 0.44 µm, with a standard deviation of 0.02 µm, and the average mass concentration is 1.71 mg/m$^3$, with a standard deviation of 0.44 mg/m$^3$. The summary of the calculations for the three days of sampling the crash recovery is displayed in Table 17.

**Table 17 Summary of MMD, CMD and mass concentration for the three days**

| | Day 1 | Day 2 | Day 3 | Average | Std Dev |
|---|---|---|---|---|---|
| Mass median diameter (µm) | 1.3927 | 1.0047 | 1.0986 | 1.1654 | 0.202418 |
| Count median diameter (µm) | 0.4362 | 0.4289 | 0.4595 | 0.4416 | 0.015981 |
| Mass concentration ($mg/m^3$) | 2.2203 | 1.4616 | 1.4489 | 1.7103 | 0.44172 |
| GM (µm) | 1.2077 | 1.1307 | 1.2238 | 1.1874 | 0.049757 |
| GSD | 1.0013 | 1.0010 | 1.0014 | 1.0012 | 0.000226 |

***SEM***

A portion of the 47-mm PTFE filter (GRIMM 1.113A, Lot 0210 11803 09036900) that was used in the PAS on the third day of aerosol sampling, when the cutting of the tail section occurred, was viewed under SEM for carbon fibers, shown in Figure 26. The SEM parameters are listed in Table 18.

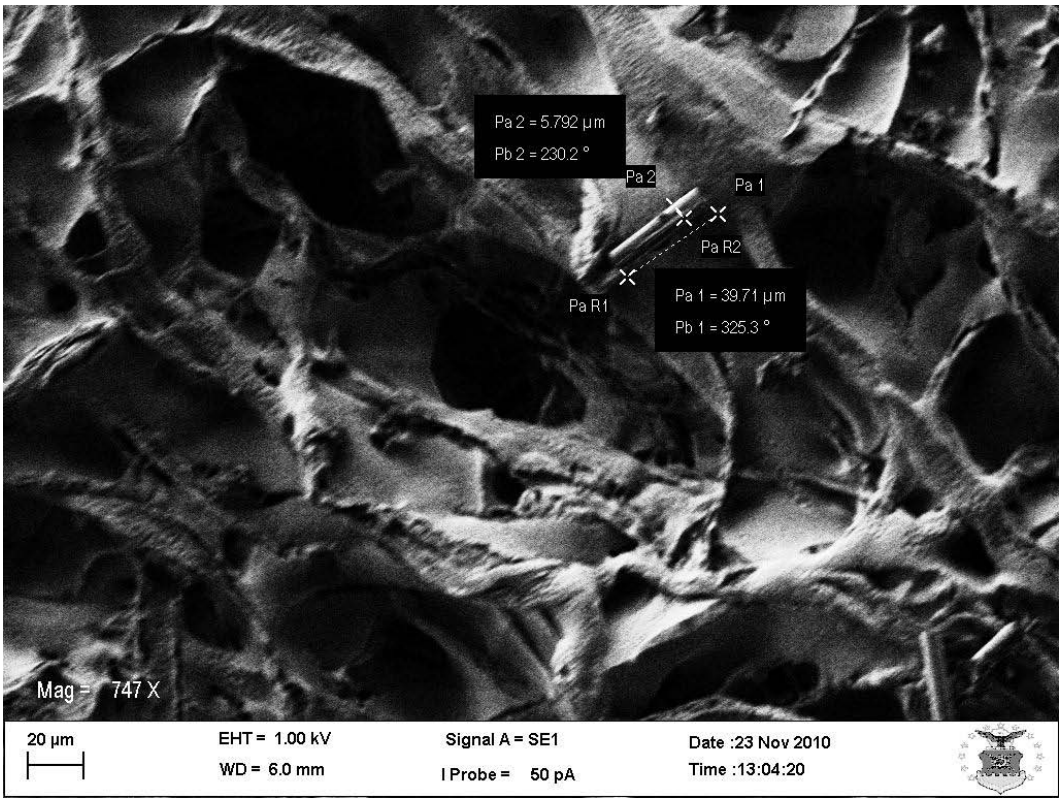


**Figure 26 SEM image of GRIMM PAS filter from C-17 crash recovery**

**Table 18 SEM condition parameters for PAS filter from C-17 crash recovery**

| Parameter | Setting |
|---|---|
| EHT | 1.0 kV |
| Working Distance | 6.0 mm |
| Beam Current | 20 pA |
| Pressure | 10 Pa |
| Aperture | Varying Pressure |

A small fiber, having an aspect ratio greater than three, was found lodged in the filter paper. Before viewing the sample, the SEM was flushed with Helium under pressure in order to remove any nitrogen or oxygen that may decompose any carbon fibers. The

fiber seen in Figure 26 is suspected to be a carbon (or graphite) fiber by the way it is illuminated, a characteristic detailed earlier in this thesis. The finding disproved the hypothesis that the PAS would not capture a carbon fiber due to the rainy conditions and spraying of wax on the debris.

## Sampling Methodology Improvements

To improve the sampling methodology, it would be necessary to ensure a surface area meter is available and operational for use in the field to provide correlational data to the CPC and OPC. When conducting aerosol sampling with the direct reading instruments, it may be helpful to take a background sample with the CPC and OPC as a baseline to be included in the statistics, or as a reference sample to compare to the other samples. In this thesis research, the background particle level was simply annotated in the laboratory notebook, as opposed to recording its own sampling period.
Because of the potential high particle concentration at the point of operation, the CPC limits of linearity would be exceeded. CPCs and OPCs are capable of providing particle counts greater than their dynamic range, which results in an estimation that is less than the true particle number concentration. Therefore, it is necessary to dilute the particles entering into the CPC or correct the raw data for this prior to performing analysis and combining with the OPC.

There are a few major variations in the ability to collect the aerosolized ultrafine particles in this research. At first, the DRIs were placed directly behind the FZ32 core milling machine in order to anticipate the worst-case scenario as the cutter would make a

pass toward the instruments. However, after seeing that the particles were being distributed out to the side of the cutter, the DRIs were moved over to the side, based on visualization. Later, it was noticed that there was a draft flowing from the back side of the booth toward the front where the operators stood. The draft was enough to direct the smaller, lighter particles in that direction, whereas, the visible heavier particles were not being affected as much by the draft. A better method would be not to try to capture the worst-case exposure, but to position the DRIs at a controlled location and leave them for the duration of the sampling collection. In this case, it may have been just as well to place them in front of the machine, between the cutter and operator's location. This was done later in the operation, but may have introduced variation in the data collection.

***SEM***

Utilizing carbon tape or a gold strip for the PTFE filter helps ensure that the electrons would not degrade, or disintegrate, the carbon fibers or carbon particulate matter. The NMAM 7400 method for viewing fibers under phase contrast microscopy returned fiber results for the conventional air sampling collection technique, but the author's analysis of the GRIMM PAS filters were not successful for fiber observation, with the exception of one fiber that may have been a carbon fiber, or simply a wood fiber from the manufacturing process of making the filter. It may be beneficial to have sent the PAS filters off to a lab for SEM analysis as done with the NMAM 7400 filters, such as a contract lab that is using computer integrated automation with the capability of scanning the entire filter sample. It would have been helpful to collect samples of bulk composite material from each field study in order to compare them to the filters under the SEM. In

addition, rather than only viewing the GRIMM PAS filters under SEM, other filters from conventional air sampling means may prove useful in showing ACM fibers.

## Answers to Research Objectives

The objectives of this research were presented in the introduction section. They are listed below with a short description of how the objectives were met in the thesis.

1. Characterize the size distribution of aerosolized particulate matter during fabrication of graphite-epoxy composite materials on B-2 panels, as well as crash and recovery operations on a C-17.

   Aerosol sampling data from the OPC and CPC were combined to create a particle size distribution for each sampling period for the B-2 panel fabrication and the crash and recovery operation for the C-17, and an average count median diameter was calculated for each size distribution.

2. Examine the feasibility of BEEs utilizing direct reading instruments at base-level to perform sampling and analysis for advanced composite materials.

   It was shown that the direct reading instruments can be taken into the field to collect aerosol sampling data that BEEs can utilize to create particle size distributions with analytical software such as *Microsoft Excel*®.

3. Ensure that current engineering controls and personnel protective equipment are adequate for workers.

   The B-2 panel fabrication sampling included data collection with the local exhaust ventilation turned on and with it turned off. The results of the particle size distributions and ANOVA of the CPC data demonstrated that the LEV significantly decreases the amount of particles aerosolized. Regarding the C-17 crash and recovery operation, the use of DRIs in the field demonstrated that immediate recommendations can be made for the use of personal protective equipment to protect the workers.

## Future Studies

As a follow-up to Capt Ferreri's bench top experiments (Ferreri, 2010), this research covered two field studies regarding the aerosolization of ACM particles. This research primarily looked at fabricating a new graphite-epoxy panel at the depot level, involving contractors and a very expensive core-milling machine that contained its own local exhaust vacuum system. It may be of great value to future research if a field study was conducted at base-level utilizing the same methodology of combining a CPC and an OPC, with the surface area meter that was left out of this thesis.

Graphite-epoxy is the advanced composite material that was studied in this research. As Ferreri points out, some USAF aircraft contain bismaleimide (BMI) as the matrix for the carbon fiber, as in the F-22 (Ferreri, 2010). Future aerosol studies may need to be conducted on the fabrication of BMI parts. For future studies, it may be beneficial to obtain as close to possible the correct density for the aerosol being sampled. An estimated density of 1.75 $g/cm^3$ was used in this thesis based on carbon composite research, but the actual value may have been somewhat higher.

As for the aircraft crash field study, methodology improvements could be made with the regards to the best placement of the direct reading instruments. It is important that they are placed out of the way so that they do not interfere with operations, but in close proximity to allow data to be recorded. However, as noted earlier, the environmental conditions and variables of the crash recovery crew (machines and equipment exhaust) will interfere with the accuracy of the data collected.

### *Future Research for the Consultant*

When responding to an aircraft crash as a consultant, it is necessary to be prepared with the supplies and equipment for conducting the aerosol sampling. The GRIMM PAS and TSI P-Trak (or other data-logging CPC) proved to be useful for field studies. A surface area meter should also be part of the equipment list for responding to an aircraft crash. The GRIMM PAS specifies the use of a PTFE filter, but it is difficult to analyze with an SEM. At the time of this research, the manufacture could not be reached to determine if another filter type, such as MCE, could be used instead. The use of a different filter in the GRIMM may prove to be a useful project for future research, either for AFIT or USAFSAM. In addition, the consultant should research the best location to place the instruments during the crash recovery operations, such as at the entry control point, downwind of the crash, or near the ACM debris.

It is also recommended to continue sampling for fibers with NMAM 7400b, which is similar to the asbestos method. This method specifies MCE filters with a pore size of 0.8 µm fixed in a 25 mm cassette with an anti-static cowl. The sampling pump airflow is to be set at 2.0 liters per minute (lpm). When sending these samples to the lab, ensure that they are marked as "fibers other than asbestos." If the type of fiber is known, write it on the sampling form. It is also recommended to sample for elemental carbon (NMAM 5040), as shown in this research. Additional air sampling includes respirable and total particulate matter, collected on pre-weighted PVC filters, to be sent to a lab that has a microbalance (6-digit scale). The PVC filters may also be used for collecting samples to be analyzed with TEM or SEM.

## Recommendations for Base-Level BEEs

Based on the literature review and the findings of this research there is not a universal recommendation for controls and personal protective equipment. The recommendations would be specific to the process occurring. However, there are some guidelines that can be followed to aid the base-level BEEs and making their recommendations. These guidelines are broken down into aircraft maintenance, crash recovery, and additional guidance for all ACM situations.

### *Aircraft Maintenance Guidance*

Spraying ACM panels down with water or wax solution during fabrication may not be feasible or may damage the material, so it is important that engineering controls are in place, such as a local exhaust ventilation (LEV) system with a HEPA filter. It is possible that fibers are aerosolized with the particulate matter as the panels are being cut. Operators should at least wear a respirator if working near the point at which fibrous particulate matter is being generated. LEV systems are shown to be effective, but they may not remove 100% of the fibrous material. The BEE should ask the operator or engineers if a wet method could be applied during the fabrication process to prevent the aerosolization of fibrous material.

Bioenvironmental Engineering (BE) flights may not have the DRIs used in this study, such as the OPC and CPC, but they should have a PORTACOUNT® that is used for gas mask fit-testing. The PORTACOUNT® can be used as a CPC, but it generally does not have the capability of logging data. It would be necessary to take good notes that include locations, times and average particle counts for background, operator

position, and place where cutting of ACM occurs. Monitor the PORTACOUNT® display for elevated particle count to determine if the ACM fabrication is generating the emission. Make PPE recommendations and other decisions to the operator to minimize possible exposure to fibrous ACM particulates.

### *Crash Recovery Guidance*

Ensure that the crash recovery crew continues to spray down ACM with a wax solution. The backpack sprayers are useful in making sure all debris is covered with the solution. If the wax solution is not immediately available, water is recommended and may be applied with a fire engine if able to get to the crash site. Initially, the crew should be wearing PPE that includes Tyvek® coveralls, gloves, boots and full-face air purifying respirator (with HEPA cartridges). The local climate conditions and crash recovery operations (e.g., hand picking debris versus using chop saw) would determine the level of PPE. For example, for the C-17 crash recovery, it was rainy and had been raining for more than 30 days. If crew members were walking around gathering debris by hand and the DRIs indicate only background level particulates, then the full PPE ensemble may be overly protective. However, on a sunny, breezy day in which it is unknown if particulate would be re-suspended, crew workers should be in full PPE.

As discussed in the *Aircraft Maintenance* Guidance, BE flights may not have the DRIs used in this study, such as the OPC and CPC, but they should have a PORTACOUNT® that is used for gas mask fit-testing. The PORTACOUNT® can be used as a CPC, but it generally does not have the capability of logging data. It would be necessary to take good notes that include locations, times and average particle counts for

background, hot zone, entry point and location where cutting of ACM occurs. If the hot zone has the same particle count as the background, the BEE may assume that particulates are not being generated from the crash site. The BEE must be constantly watching the display on the DRI for sudden shifts in particle count and act quickly to determine the source of emission. More wax or water should be added to the debris if it is determined that particulates are being stirred up or generated from cutting and removing ACM.

### *Additional Sampling Guidance for all ACM Situations*

In addition to the direct reading instruments, BEEs should be performing integrated personnel air sampling. It is recommended to continue sampling for fibers with NMAM 7400b, similar to the asbestos method. This method specifies MCE filters with a pore size of 0.8 µm fixed in a 25 mm cassette with an anti-static cowl. The sampling pump airflow is to be set at 2.0 liters per minute (lpm). When sending these samples to the lab, ensure that they are marked as "fibers other than asbestos." If the type of fiber is known, write it on the sampling form. It is also recommended to sample for elemental carbon (NMAM 5040), as mentioned earlier in this research. Additional air sampling includes respirable and total particulate matter, collected on pre-weighted PVC filters, to be sent to a lab that has a microbalance (6-digit scale). The PVC filters may also be used for collecting samples to be analyzed with TEM or SEM.

# V. Conclusions

The primary purpose of this research was to follow up on Capt Ferreri's thesis on carbon fiber characterization, because ACM is becoming more prevalent on USAF aircraft and may pose a future health hazard for Air Force members performing work on them. Ferreri's research occurred on bench top and concluded that more research was needed for field studies to better understand aerosol behavior of advanced composite material during fabrication operations, including burnt ACM, and to determine the sufficiency of engineering controls. Two field studies were conducted for this thesis in order to characterize ACM aerosol size distribution, determine the feasibility of utilizing DRIs in the field, and ensure workers are protected with adequate controls. Although the majority of the research is on fabrication of newly designed graphite-epoxy panels, the latter part discusses using DRIs during a response to an aircraft crash.

One of the research objectives was to gain understanding of the particle size characteristics of the ACM as it is aerosolized during cutting and drilling operations. In order to characterize exposure, traditional integrated air sampling was positioned together near an ACM panel as it was cut with a core milling machine. Gravimetric analyses and fiber counts were conducted on the integrated samples. The 37-mm filter, which is currently used as the standard for aerosol sampling of particulate matter, resulted in the least mass concentration. Particle counts and size distributions were analyzed using the DRIs (optical and condensation particle counters).

The focus of the field experiments with the DRIs was to combine the data from the OPC and CPC to create one particle size distribution to be used for ensuring current

engineering controls are adequate. Statistics revealed a significant decrease (F-value < 0.0001) in the particle count for respirable sized ultra-fine particles when the local exhaust ventilation was turned on. The second field study, which involved utilizing the DRIs during a C-17 crash and recovery operation, proved that the OPCs and CPCs can be helpful for base-level bioenvironmental engineers (BEEs) for recommending personal protective equipment for the clean-up crew.

This research showed that real-time use of the DRIs in the field can provide the base-level BEEs a cost-effective and time saving tool that can aid in determining the emission source of ACM, or other ultrafine particles, and recommending immediate engineering or administrative controls. The results show whether or not the current engineering controls in place are adequate. As a result of this research, controls, policies, and procedures can be implemented across all Air Force installations where there is a concern for ACM exposure to structural maintenance workers.

# Appendix A

The gravimetric analyses, the measured mass collected on the filters, are displayed in Tables 15-17. The results of the mass measured are less than the required LOQ, invalidating the gravimetric analyses. Therefore, the gravimetrical analysis did not prove useful.

**Table 19 Gravimetric results for Total Particulate Mass**

| Total Particulate Mass | | | |
|---|---|---|---|
| | Pre-weight (g) | Post-weight (g) | Avg Diff (g) |
| **1** | 0.0169 | 0.0176 | |
| | 0.0169 | 0.0175 | |
| | 0.0169 | 0.0175 | |
| avg: | 0.0169 | 0.0175 | 0.0006 |
| std: | 0.0000 | 0.0001 | |
| **2** | 0.0138 | 0.0140 | |
| | 0.0136 | 0.0141 | |
| | 0.0137 | 0.0141 | |
| avg: | 0.0137 | 0.0141 | 0.0004 |
| std: | 0.0001 | 0.0001 | |
| **3** | 0.0135 | 0.0142 | |
| | 0.0135 | 0.0141 | |
| | 0.0136 | 0.0142 | |
| avg: | 0.013533333 | 0.0142 | 0.0006 |
| std: | 0.0001 | 0.0001 | |
| **4** | 0.0141 | 0.0148 | |
| | 0.0144 | 0.0149 | |
| | 0.0143 | 0.0148 | |
| avg: | 0.014266667 | 0.0148 | 0.0006 |
| std: | 0.0002 | 0.0001 | |
| **5** | 0.0164 | 0.0166 | |
| | 0.0163 | 0.0167 | |
| | 0.0164 | 0.0166 | |
| avg: | 0.016366667 | 0.0166 | 0.0003 |
| std: | 0.0001 | 0.0001 | |

| | | | |
|---|---|---|---|
| **6** | 0.0154 | 0.0158 | |
| | 0.0154 | 0.0157 | |
| | 0.0154 | 0.0157 | |
| avg: | 0.0154 | 0.0157 | 0.0003 |
| std: | 0.0000 | 0.0001 | |
| **7** | 0.0127 | 0.0166 | |
| | 0.0127 | 0.0166 | |
| | 0.0127 | 0.0167 | |
| avg: | 0.0127 | 0.0166 | 0.0039 |
| std: | 0.0000 | 0.0001 | |
| (Req'd LOQ = 0.001528g) | | Total Avg mass: | 0.0010 |
| | | Total Avg mass st dev: | 0.001319 |

**Table 20 Gravimetric results for Respirable Particulate Mass**

**Respirable Particulate Mass**

| | Pre-weight (g) | Post-weight (g) | Avg Diff (g) |
|---|---|---|---|
| **11** | 0.0135 | 0.0137 | |
| | 0.0137 | 0.0138 | |
| | 0.0135 | 0.0137 | |
| avg: | 0.013566667 | 0.0137 | 0.0002 |
| std: | 0.0001 | 0.0001 | |
| **12** | 0.0141 | 0.0141 | |
| | 0.014 | 0.0142 | |
| | 0.0141 | 0.0142 | |
| avg: | 0.014066667 | 0.0142 | 0.0001 |
| std: | 0.0001 | 0.0001 | |
| **13** | 0.0134 | 0.0136 | |
| | 0.0135 | 0.0134 | |
| | 0.0135 | 0.0135 | |
| avg: | 0.013466667 | 0.0135 | 0.0000 |
| std: | 0.0001 | 0.0001 | |
| **14** | 0.0153 | 0.0155 | |
| | 0.0153 | 0.0153 | |
| | 0.0153 | 0.0154 | |
| avg: | 0.0153 | 0.0154 | 0.0001 |
| std: | 0.0000 | 0.0001 | |
| **15** | 0.0139 | 0.0138 | |

| | | | |
|---|---|---|---|
| | 0.0138 | 0.0138 | |
| | 0.0139 | 0.0139 | |
| avg: | 0.013866667 | 0.0138 | 0.0000 |
| std: | 0.0001 | 0.0001 | |
| **16** | 0.016 | 0.0162 | |
| | 0.016 | 0.0162 | |
| | 0.0161 | 0.0160 | |
| avg: | 0.016033333 | 0.0161 | 0.0001 |
| std: | 0.0001 | 0.0001 | |
| **17** | 0.0148 | 0.0157 | |
| | 0.0149 | 0.0158 | |
| | 0.0148 | 0.0157 | |
| avg: | 0.014833333 | 0.0157 | 0.0009 |
| std: | 0.0001 | 0.0001 | |
| (Req'd LOQ = 0.001155g) | | Respirable Avg mass: | 0.000195 |
| | | Respirable Avg mass std dev: | 0.000317 |

**Table 21 Gravimetric results for GRIMM PAS filters**

| 47 mm PTFE filter for Grimm | | | |
|---|---|---|---|
| | | | |
| | **Pre-weight (g)** | **Post-weight (g)** | **Avg Diff (g)** |
| **1** | 0.3098 | 0.3099 | |
| | 0.3098 | 0.3100 | |
| | 0.3098 | 0.3100 | |
| avg: | 0.3098 | 0.3100 | 0.0002 |
| std dev: | 0.0000 | 0.0001 | |
| **2** | 0.3112 | 0.3118 | |
| | 0.3111 | 0.3120 | |
| | 0.3111 | 0.3120 | |
| avg: | 0.3111 | 0.3119 | 0.0008 |
| std dev: | 0.0001 | 0.0001 | |
| | | Avg mass std: | 0.000448 |
| (Req'd LOQ > 0.001155g) | | LOQ for avg: | 0.00447834 |

# Appendix B

## *CPC Charts for Cutting of B-2 Panels*

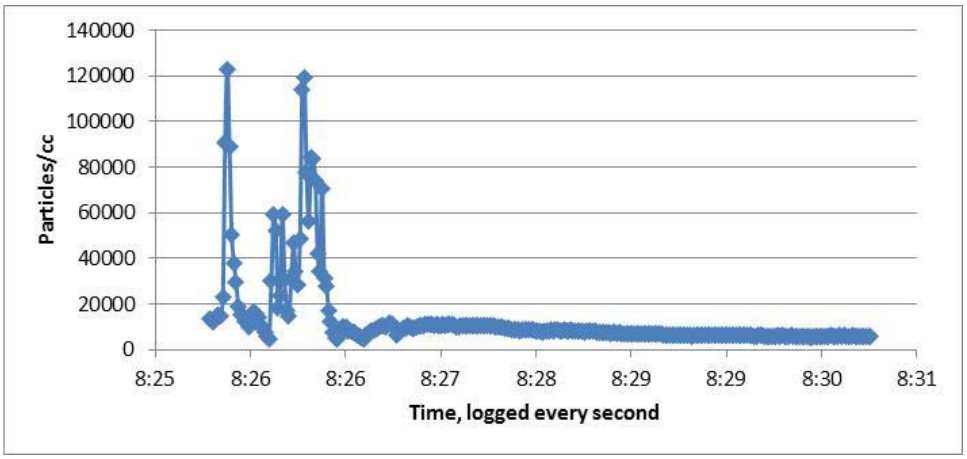


**Figure 27 CPC particle count for DAY 1b of B-2 panel cutting**

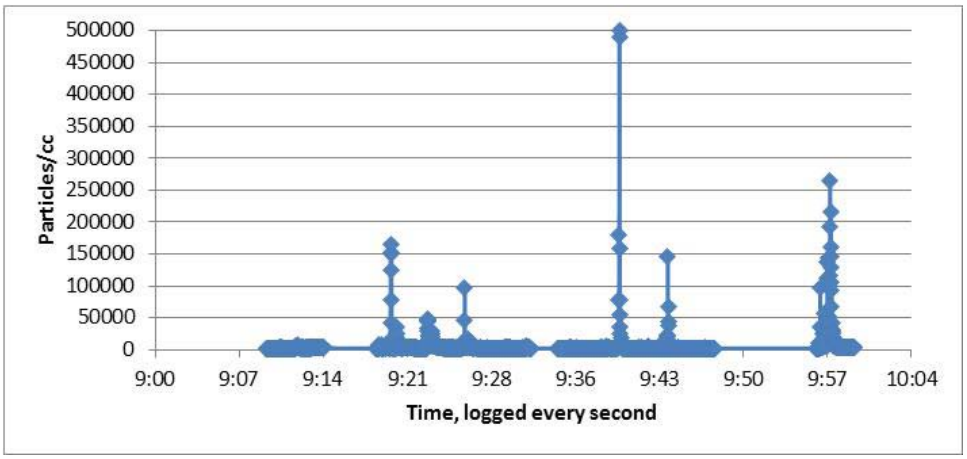


**Figure 28 CPC particle count for DAY 1c of B-2 panel cutting**

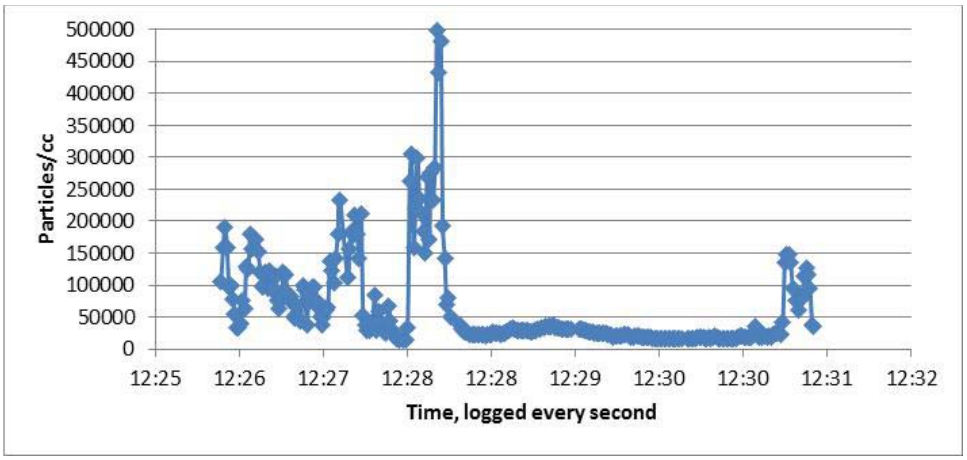


**Figure 29 CPC particle count for DAY 1c of B-2 panel cutting**

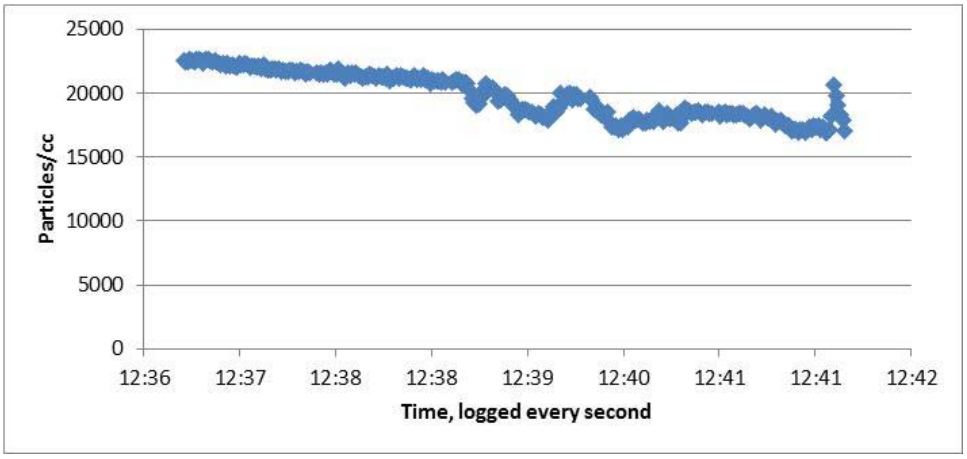


**Figure 30 CPC particle count for DAY 1e of B-2 panel cutting**

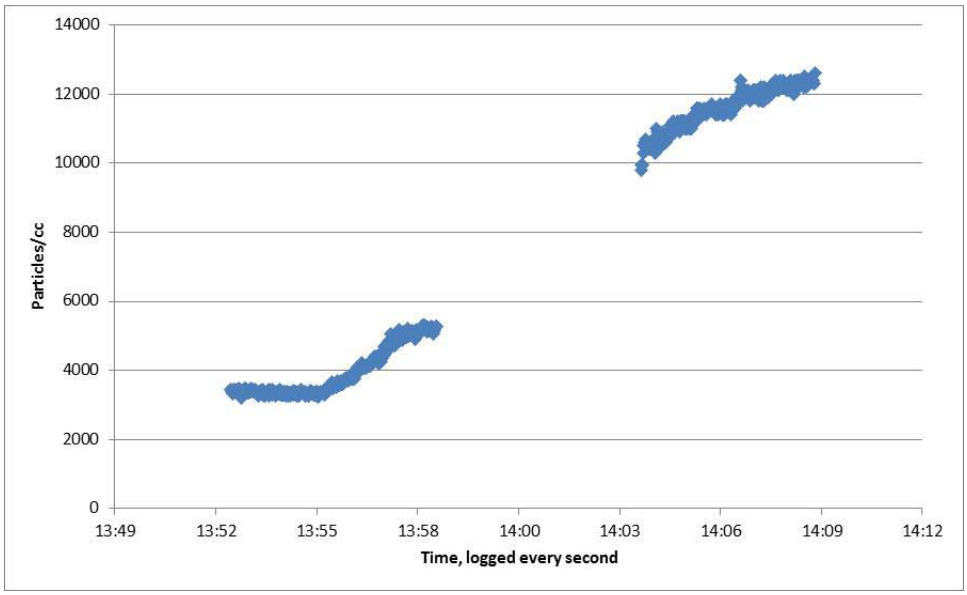


**Figure 31 CPC particle count for DAY 1f of B-2 panel cutting**

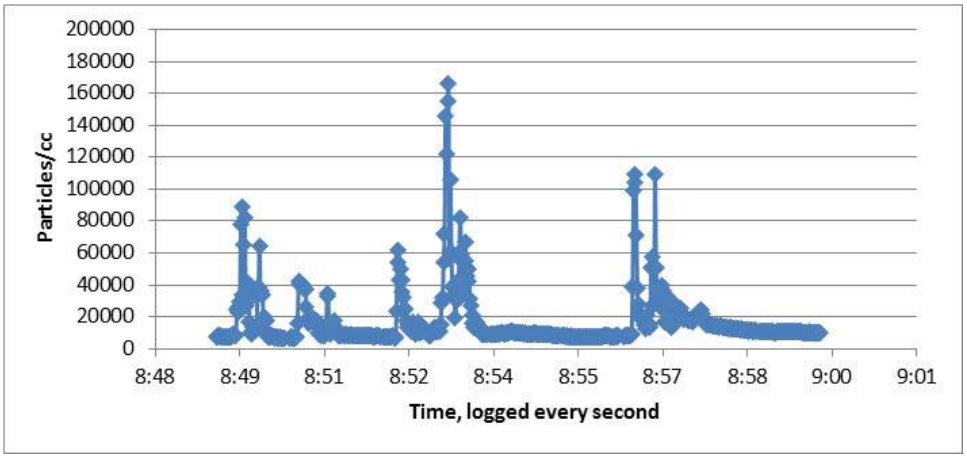


**Figure 32 CPC particle count for DAY 2a of B-2 panel cutting**

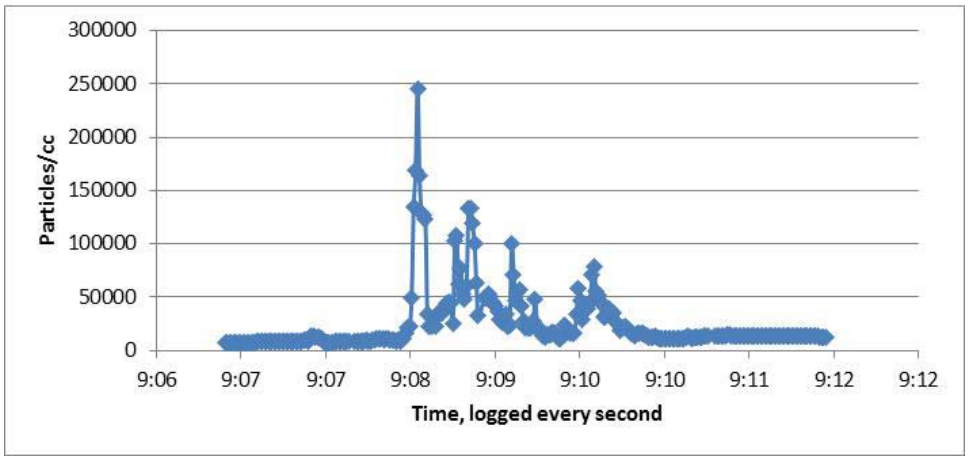


**Figure 33 CPC particle count for DAY 2b of B-2 panel cutting**

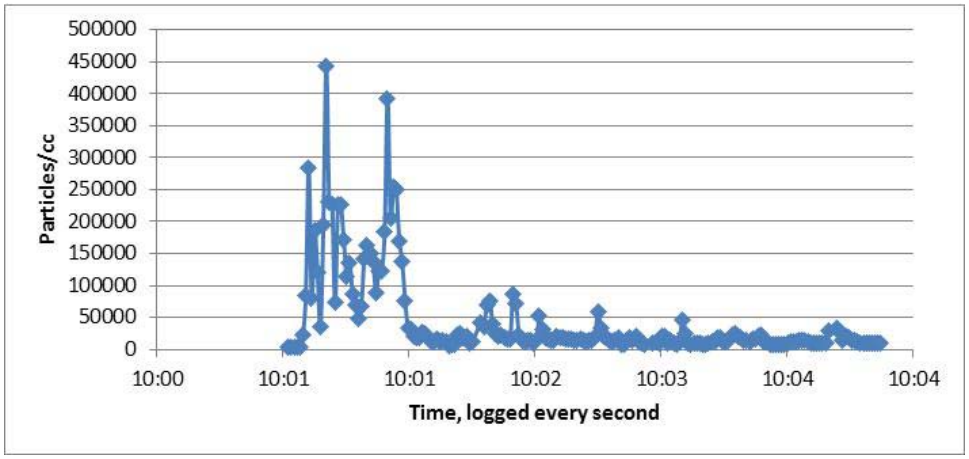


**Figure 34 CPC particle count for DAY 2c of B-2 panel cutting**

# Appendix C

## Justification of Log-Normal CPC Data

### *JMP 8.0® Output for CPC Raw Data Distribution*

**(**This is for the combined sampling prior to splitting into time periods)

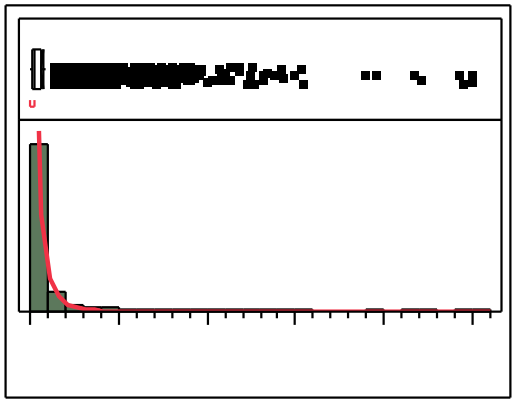

LogNormal(8.80078,1.06794)

**Quantiles**

| | | |
|---|---|---|
| 100.0% | maximum | 500000 |
| 99.5% | | 221570 |
| 97.5% | | 97855 |
| 90.0% | | 24500 |
| 75.0% | quartile | 12200 |
| 50.0% | median | 6100 |
| 25.0% | quartile | 2470 |
| 10.0% | | 2030 |
| 2.5% | | 1602 |
| 0.5% | | 1294 |
| 0.0% | minimum | 1220 |

**Moments**

| | |
|---|---|
| Mean | 14150.432 |
| Std Dev | 31837.438 |
| Std Err Mean | 408.13874 |
| Upper 95% Mean | 14950.529 |
| Lower 95% Mean | 13350.336 |
| N | 6085 |

**Fitted LogNormal**

**Parameter Estimates**

| Type | Parameter | Estimate | Lower 95% | Upper 95% |
|---|---|---|---|---|
| Scale | μ | 8.8007844 | 8.7739475 | 8.8276213 |
| Shape | σ | 1.0679371 | 1.0492409 | 1.0871953 |

***JMP® Output for CPC Day 1a***

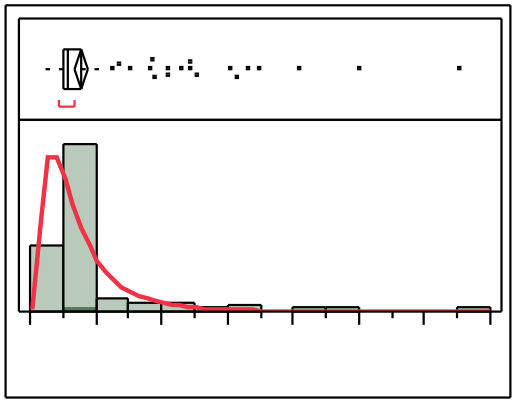

LogNormal(8.67765,0.7326)

## Quantiles

| | | |
|---|---|---|
| 100.0% | maximum | 65400 |
| 99.5% | | 65400 |
| 97.5% | | 33140 |
| 90.0% | | 12510 |
| 75.0% | quartile | 7695 |
| 50.0% | median | 5715 |
| 25.0% | quartile | 5000 |
| 10.0% | | 1489 |
| 2.5% | | 1300 |
| 0.5% | | 1250 |
| 0.0% | minimum | 1250 |

## Moments

| | |
|---|---|
| Mean | 7807.1717 |
| Std Dev | 7909.99 |
| Std Err Mean | 562.13851 |
| Upper 95% Mean | 8915.7533 |
| Lower 95% Mean | 6698.5901 |
| N | 198 |

## Fitted LogNormal
## Parameter Estimates

| Type | Parameter | Estimate | Lower 95% | Upper 95% |
|---|---|---|---|---|
| Scale | μ | 8.6776482 | 8.575108 | 8.7801884 |
| Shape | σ | 0.7326031 | 0.6659685 | 0.8111383 |

***JMP® Output for CPC Day 1b***

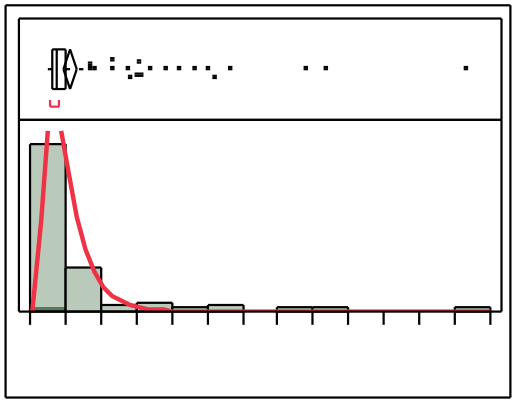

LogNormal(9.08663,0.55663)

## Quantiles

| | | |
|---|---|---|
| 100.0% | maximum | 123000 |
| 99.5% | | 123000 |
| 97.5% | | 52110 |
| 90.0% | | 17110 |
| 75.0% | quartile | 10100 |
| 50.0% | median | 7585 |
| 25.0% | quartile | 6140 |
| 10.0% | | 5899 |
| 2.5% | | 5545 |
| 0.5% | | 4670 |
| 0.0% | minimum | 4670 |

## Moments

| | |
|---|---|
| Mean | 11284.697 |
| Std Dev | 13480.902 |
| Std Err Mean | 958.04601 |
| Upper 95% Mean | 13174.039 |
| Lower 95% Mean | 9395.3545 |
| N | 198 |

## Fitted LogNormal
## Parameter Estimates

| Type | Parameter | Estimate | Lower 95% | Upper 95% |
|---|---|---|---|---|
| Scale | μ | 9.0866308 | 9.0087204 | 9.1645412 |
| Shape | σ | 0.5566344 | 0.5060052 | 0.6163057 |

***JMP® Output for CPC Day 1c***

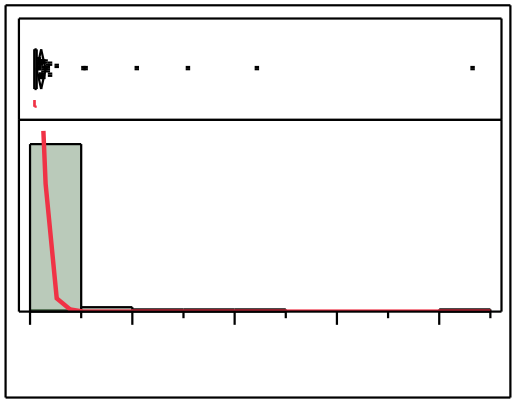

LogNormal(7.95871,0.67489)

## Quantiles

| | | |
|---|---|---|
| 100.0% | maximum | 216000 |
| 99.5% | | 216000 |
| 97.5% | | 27835 |
| 90.0% | | 5453 |
| 75.0% | quartile | 2825 |
| 50.0% | median | 2340 |
| 25.0% | quartile | 2058 |
| 10.0% | | 1937 |
| 2.5% | | 1789 |
| 0.5% | | 1650 |
| 0.0% | minimum | 1650 |

## Moments

| | |
|---|---|
| Mean | 5332.0707 |
| Std Dev | 18237.494 |
| Std Err Mean | 1296.0823 |
| Upper 95% Mean | 7888.0474 |
| Lower 95% Mean | 2776.094 |
| N | 198 |

## Fitted LogNormal
## Parameter Estimates

| Type | Parameter | Estimate | Lower 95% | Upper 95% |
|---|---|---|---|---|
| Scale | μ | 7.9587092 | 7.8642466 | 8.0531719 |
| Shape | σ | 0.6748926 | 0.6135071 | 0.7472412 |

***JMP® Output for CPC Day 1d***

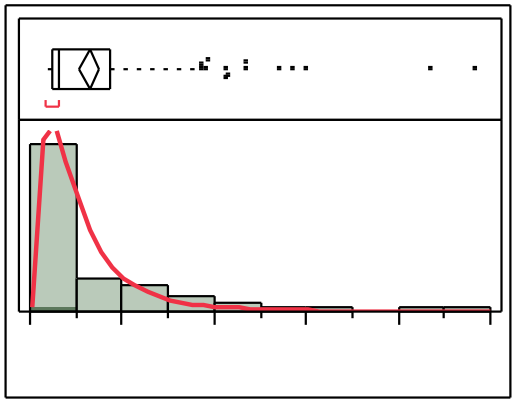

LogNormal(10.6742,0.81339)

**Quantiles**

| | | |
|---|---|---|
| 100.0% | maximum | 484000 |
| 99.5% | | 484000 |
| 97.5% | | 270400 |
| 90.0% | | 156000 |
| 75.0% | quartile | 87350 |
| 50.0% | median | 31600 |
| 25.0% | quartile | 23275 |
| 10.0% | | 18900 |
| 2.5% | | 17900 |
| 0.5% | | 15300 |
| 0.0% | minimum | 15300 |

**Moments**

| | |
|---|---|
| Mean | 64114.141 |
| Std Dev | 71367.877 |
| Std Err Mean | 5071.8941 |
| Upper 95% Mean | 74116.318 |
| Lower 95% Mean | 54111.965 |
| N | 198 |

**Fitted LogNormal**
**Parameter Estimates**

| Type | Parameter | Estimate | Lower 95% | Upper 95% |
|---|---|---|---|---|
| Scale | μ | 10.674215 | 10.560368 | 10.788063 |
| Shape | σ | 0.8133917 | 0.7394088 | 0.9005874 |

***JMP® Output for CPC Day 1e***

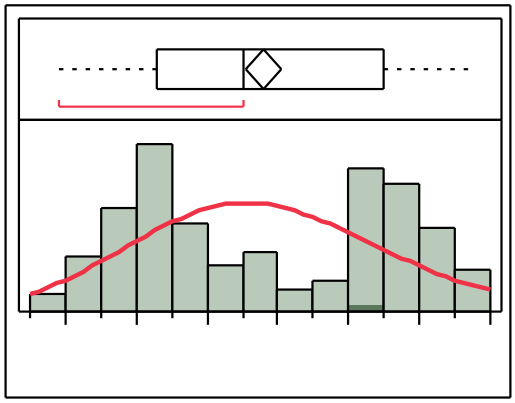

LogNormal(9.88914,0.08938)

## Quantiles

| | | |
|---|---|---|
| 100.0% | maximum | 22700 |
| 99.5% | | 22700 |
| 97.5% | | 22600 |
| 90.0% | | 22110 |
| 75.0% | quartile | 21500 |
| 50.0% | median | 19500 |
| 25.0% | quartile | 18300 |
| 10.0% | | 17700 |
| 2.5% | | 17098 |
| 0.5% | | 16900 |
| 0.0% | minimum | 16900 |

## Moments

| | |
|---|---|
| Mean | 19793.939 |
| Std Dev | 1771.4211 |
| Std Err Mean | 125.88941 |
| Upper 95% Mean | 20042.203 |
| Lower 95% Mean | 19545.676 |
| N | 198 |

## Fitted LogNormal

## Parameter Estimates

| Type | Parameter | Estimate | Lower 95% | Upper 95% |
|---|---|---|---|---|
| Scale | μ | 9.8891402 | 9.8766304 | 9.90165 |
| Shape | σ | 0.0893769 | 0.0812475 | 0.0989581 |

***JMP® Output for CPC Day 1f***

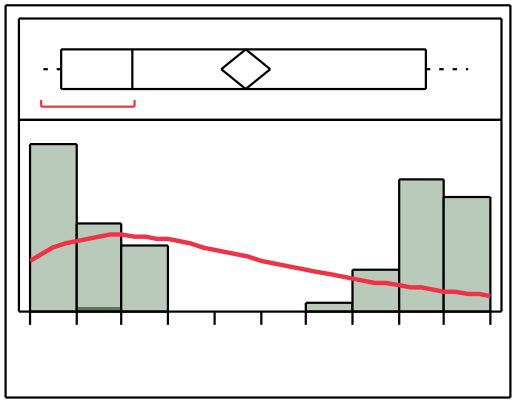

LogNormal(8.8032,0.54921)

**Quantiles**

| | | |
|---|---|---|
| 100.0% | maximum | 12500 |
| 99.5% | | 12500 |
| 97.5% | | 12400 |
| 90.0% | | 12200 |
| 75.0% | quartile | 11600 |
| 50.0% | median | 5240 |
| 25.0% | quartile | 3698 |
| 10.0% | | 3360 |
| 2.5% | | 3270 |
| 0.5% | | 3190 |
| 0.0% | minimum | 3190 |

**Moments**

| | |
|---|---|
| Mean | 7678.7879 |
| Std Dev | 3847.4185 |
| Std Err Mean | 273.42413 |
| Upper 95% Mean | 8218.0019 |
| Lower 95% Mean | 7139.5739 |
| N | 198 |

**Fitted LogNormal**
**Parameter Estimates**

| Type | Parameter | Estimate | Lower 95% | Upper 95% |
|---|---|---|---|---|
| Scale | μ | 8.8031999 | 8.7263286 | 8.8800713 |
| Shape | σ | 0.5492109 | 0.4992569 | 0.6080863 |

***JMP® Output for CPC Day 2a***

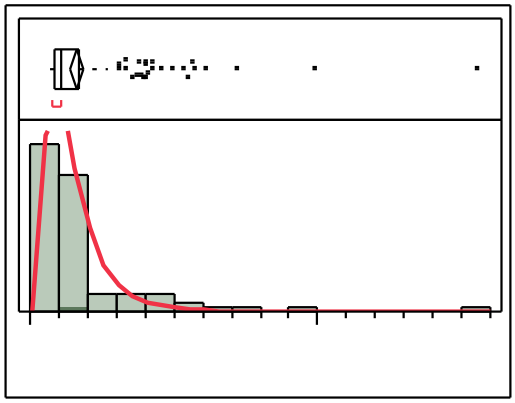

LogNormal(9.44987,0.60263)

## Quantiles

| | | |
|---|---|---|
| 100.0% | maximum | 155000 |
| 99.5% | | 155000 |
| 97.5% | | 57303 |
| 90.0% | | 37470 |
| 75.0% | quartile | 16650 |
| 50.0% | median | 10500 |
| 25.0% | quartile | 8178 |
| 10.0% | | 7505 |
| 2.5% | | 6740 |
| 0.5% | | 6570 |
| 0.0% | minimum | 6570 |

## Moments

| | |
|---|---|
| Mean | 16203.838 |
| Std Dev | 16590.277 |
| Std Err Mean | 1179.0196 |
| Upper 95% Mean | 18528.958 |
| Lower 95% Mean | 13878.718 |
| N | 198 |

## Fitted LogNormal
## Parameter Estimates

| Type | Parameter | Estimate | Lower 95% | Upper 95% |
|---|---|---|---|---|
| Scale | μ | 9.4498724 | 9.3655244 | 9.5342205 |
| Shape | σ | 0.6026285 | 0.5478159 | 0.6672304 |

***JMP® Output for CPC Day 2b***

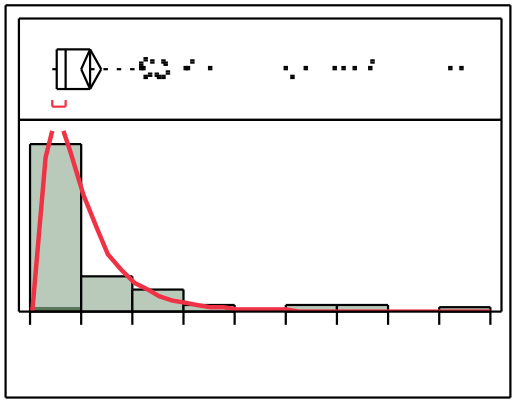

LogNormal(9.72408,0.72882)

**Quantiles**

| | | |
|---|---|---|
| 100.0% | maximum | 169000 |
| 99.5% | | 169000 |
| 97.5% | | 127150 |
| 90.0% | | 49740 |
| 75.0% | quartile | 23075 |
| 50.0% | median | 13600 |
| 25.0% | quartile | 10060 |
| 10.0% | | 8181 |
| 2.5% | | 7509 |
| 0.5% | | 7370 |
| 0.0% | minimum | 7370 |

**Moments**

| | |
|---|---|
| Mean | 23725.051 |
| Std Dev | 27851.677 |
| Std Err Mean | 1979.3325 |
| Upper 95% Mean | 27628.451 |
| Lower 95% Mean | 19821.65 |
| N | 198 |

**Fitted LogNormal**

**Parameter Estimates**

| Type | Parameter | Estimate | Lower 95% | Upper 95% |
|---|---|---|---|---|
| Scale | μ | 9.7240796 | 9.6220688 | 9.8260903 |
| Shape | σ | 0.7288202 | 0.6625297 | 0.8069499 |

***JMP® Output for CPC Day 2c***

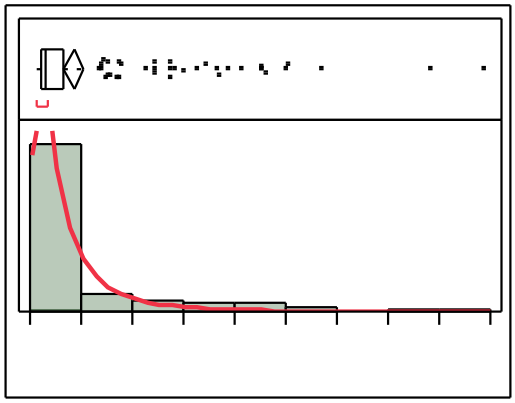

LogNormal(9.98501,1.0285)

## Quantiles

| | | |
|---|---|---|
| 100.0% | maximum | 443000 |
| 99.5% | | 443000 |
| 97.5% | | 249100 |
| 90.0% | | 137100 |
| 75.0% | quartile | 31800 |
| 50.0% | median | 15450 |
| 25.0% | quartile | 11250 |
| 10.0% | | 8499 |
| 2.5% | | 3488 |
| 0.5% | | 3360 |
| 0.0% | minimum | 3360 |

## Moments

| | |
|---|---|
| Mean | 42960 |
| Std Dev | 68112.949 |
| Std Err Mean | 4840.5765 |
| Upper 95% Mean | 52505.999 |
| Lower 95% Mean | 33414.001 |
| N | 198 |

## Fitted LogNormal
## Parameter Estimates

| Type | Parameter | Estimate | Lower 95% | Upper 95% |
|---|---|---|---|---|
| Scale | μ | 9.9850112 | 9.8410556 | 10.128967 |
| Shape | σ | 1.0284977 | 0.9349497 | 1.1387528 |

# Bibliography


Agency for Toxic Substances and Disease Registry. (2002). *Technical Briefing Paper: Health effects from exposure to fibrous glass, rock wool, or slag wool.* U.S. Department of Health and Human Services, Public Health Service.

Araujo, J. A., & Nel, A. E. (2009). Particulate matter and atherosclerosis: role of particle size, composition and oxidative stress. *Particle & Fibre Toxicology*.

Boeing. (2005, July 6). *Defense, Space and Security*. Retrieved January 21, 2011, from F-22 Raptor Aft Fuselage Facts: http://www.boeing.com/defense-space/military/f22/f22facts.html

Brown, L. M., Collings, N., Harrison, R. M., Maynard, A. D., & Maynard, R. L. (2003). *Ultrafine Particles in the Atmosphere.* London, UK: Imperial College Press.

Brunekreef, B., & Forsberg, B. (2005). Epidemiological evidence of effects of coarse airborne particles on health. *European Respiratory Journal*, 309-318.

Donaldson, K., Li, X. Y., & MacNee, W. (1998). Ultrafine (nanometer) particle mediated lung injury. *Journal of Aerosol Science*, 553-560.

F. Zimmermann GmbH. (2007, August). *Zimmermann Portal Milling Machines*. Retrieved January 4, 2011, from Zimmermann: http://www.f-zimmermann.com/fileadmin/Mediendatenbank/Subnavi/Produkte/CNC/PDFs_FZ_Maschinen/Englisch/FZ32_e.pdf

Ferreri, M. (2010, Mar). Particulate Characterization and Control Evaluation for Carbon Fiber Composite Aircraft Crash Recovery Operations. Air Force Institute of Technology.

Ferreri, M., Slagley, J., & Felker, D. (2009). Characterization of Advanced Composite Material Particles Released During Simulated Crash Recovery Operations. *AIHce.* Toronto.

Gandhi, S., Lyon, R., & Speitel, L. (1999). Potential Health Hazards from Burning Aircraft Composites. *Journal of Fire Sciences, 17*, 20-41.

GRIMM Aerosol Technik GmbH & Co. (2009). Portable Laser Aerosolspectrometer and Dust Monitor Model 1.108/1.109. *GRIMM Aerosol Technik GmbH & Co. KG*. Germany: GRIMM Aerosol Technik, Ainring.

Heitbrink, W. A., Evans, D. E., Ku, B. K., Maynard, A. D., Slavin, T. J., & Peters, T. M. (2009). Relationships Among Particle Number, Surface Area, and Respirable Mass Concentration in Automotive Engine Manufacturing. *Journal of Occupational and Environmental Hygiene, 6*(1), 19-31.

Hinds, W. C. (1999). *Aerosol Technology: Properties, behavior, and measurement of airborne particles second edition.* New York: John Wiley and Sons, inc.

ISO. (1995). Air Quality - Particle size fraction definitions for health-related sampling. *International Standards Organization.* Geneva: ISO 7708.

Kalpakjian, S., & Schmid, S. (2001). *Manufacturing Engineering and Technology.* Upper Saddle River: Prentice Hall.

Lademann, J., Weigmann, H., Rickmeyer, C., Barthelmes, H., Schaefer, H., Mueller, G., et al. (1999). Penetration of titanium dioxide microparticles in a sunscreen formulation into the horny layer and the follicular orifice. *Skin Pharmacol Appl Skin Physiol*, 247-256.

LeBlancab, A. J., Cumpstonc, J. L., Chenc, B. T., Frazerbc, D., Castranovac, V., & Nurkiewiczabd, T. R. (2009). Nanoparticle inhalation impairs endothelium-dependent vasodilation in subepicardial arterioles. *Journal of Toxicology and Environmental Health*, 1576-1584.

Li, N., Sioutas, C., Cho, A., Schmitz, D., Misra, C., Sempf, J., et al. (2003). Ultrafine particulate induce oxidative stress and mitochondrial damage. *Environmental Health Perspectives*, 455-460.

Martin, T. R., Meyer, S. W., & Luchtel, D. R. (1989). An evaluation of the toxicity of carbon fiber composites for lung cells in vitro and in vivo. *Environmental Research*, 246-261.

Maynard, A. D. (2006). Nanotechnology: The Next Big Thing, or Much Ado about Nothing. *Annals of Occupational Hygiene, 51*(1), 1-12.

Maynard, A. D., & Kuempel, E. D. (2005). Airborne nanostructured particles and occupational health. *Journal of Nanoparticle Research, 7*, 587-614.

McClellan, R. O. (2002). Setting ambient air quality standards for particulate matter. *Toxicology 181*, 329-347.

Methner, M., Hodson, L., & Geraci, C. (2010). Nanoparticle Emission Assessment Technique (NEAT) for the Identification and Measurement of Potential Inhalation Exposures to Engineered Nanomaterials - Part A. *Journal of Occupational and Environmental Hygiene, 7*(3), 127-132.

Methner, M., Hodson, L., Dames, A., & Geraci, C. (2010). Nanoparticle Emission Assessment Technique (NEAT) for the Identification and Measurement of Potential Inhalation Exposures to Engineered Nanomaterials - Part B: Results from 12 Field Studies. *Journal of Occupational and Environmental Hygiene, 7*(3), 163-176.

Ness, S. A. (1991). *Air Monitoring for Toxic Exposures.* New York: Van Nostrand Reinhold.

NIOSH. (2010, September). *CDC - NIOSH.* Retrieved from NIOSH Pocket Guide to Chemical Hazards - Particulates not otherwise regulated: http://www.cdc.gov/niosh/npg/npgd0480.html

Oberdörster, G. (1996). Significance of particle parameters in the evaluation of exposure-dose-response relationships of inhaled particles. *Inhalation Toxicology*, 73-89.

Oberdörster, G., & Utell, M. J. (2002). Ultrafine particles in the urban air: to the respiratory tract-and beyond. *Environmental Health Perspectives*, A440-A441.

Oberdörster, G., Maynard, A., Donaldson, K., Castranova, V., Fitzpatrick, J., Ausman, K., et al. (2005). Principles for characterizing the potential human health effects from exposure to nanomaterials: elements of a screening strategy. *Particle and Fibre Toxicology, 2*(8).

Oberdörster, G., Oberdörster, E., & Oberdörster, J. (2005). Nanotoxicology: An Emerging Discipline Evolving from Studies of Ultrafine Particles. *Environmental Health Perspectives, 113*(7), 823-839.

Oberdörster, G., Sharp, Z., Atudorei, V., Elder, A., Gelein, R., Kreyling, W., et al. (2004). Translocation of Inhaled Ultrafine Particles to the Brain. *Inhalation Toxicology, 16*(6-7), 437-445.

Occupational Safety & Health Administration. (1999, January 20). *OSHA Technical Manual (OTM) - Section III: Chapter 1: Polymer Matrix Materials: Advanced Composites.* Retrieved January 19, 2011, from OSHA Technical Manual: http://www.osha.gov/dts/osta/otm/otm_iii/otm_iii_1.html

Puett, R. C., Hart, J. E., Yanosky, J. D., Paciorek, C., Schwartz, J., Suh, H., et al. (2009). Chronic Fine and Coarse Particulate Exposure, Mortality, and Coronary Heart Disease in the Nurses' Health Study. *Environmental Health Perspectives*, 1702-1706.

Sager, T. M., & Castranova, V. (2009). Surface area of particle administered versus mass in determining the pulmonary toxicity of ultrafine and fine carbon black: comparison to ultrafine titanium dioxide. *Particle and Fibre Toxicology*.

Schmoll, L. H., Peters, T. M., & O'Shaughnessy, P. T. (2010). Use of a Condensation Particle Counter and an Optical Particle Counter to Assess the Number Concentration of Engineered Nanoparticles. *Journal of Occupational and Environmental Hygiene*, 535-545.

Thomson, S. A. (1989). Proceedings Occupational Health Aspects of Advanced Composite Technology in the Aerospace Industry, Health Effects and Exposure Considerations. *Toxicology of Carbon Fibers*, (pp. 164-176).

Tinkle, S. S., Antonini, J. M., Rich, B. A., Roberts, J. R., Salmen, R., DePree, K., et al. (2003). Skin as a Route of Exposure and Sensitization in Chronic Beryllium Disease. *Environmental Health Perspectives, 111*(9), 1201-1208.

TSI. (2006, June). *P-Trak Ultrafine Particle Counter Theory of Operation.* Retrieved January 3, 2010, from Indoor Air Quality: http://www.tsi.com/documents/ITI-071.pdf

TSI. (2007). *Ptrak 8525 specification sheet.* Retrieved from TSI: http://www.tsi.com/uploadedFiles/Product_Information/Literature/Spec_Sheets/PTrakSpec2980453.pdf

Viswanathan, H., Rooke, M. A., & Sherwood, P. M. (1997). X-Ray photoelectric spectroscopic studies of carbon-fiber surfaces. 21. Comparison of carbon fibers

electrochemically oxidized in acid using achromatic and monochromatic XPS. *Surface and Interface Analysis*, 409-417.

Warheit, D. B., Hansen, J. F., Carakostas, M. C., & Hartsky, M. A. (1994). Acute inhalation toxicity studies in rats with a respirable-sized experimental carbon fiber: pulmonary biochemical and cellular effects. *American Occupational Hygiene*, 769-776.

Warheit, D. B., Hoke, R. A., Finlay, C., Donner, E. M., Reed, K. L., & Sayes, C. M. (2007). Development of a base set of toxicity tests using ultrafine TiO2 particles as a component of nanoparticle risk management. *Toxicology Letters, Vol 171, Issue 3*, 99-110.

Wilson, W. E., Stanek, J., Han, H.-S., Johnson, T., Sakurai, H., Pui, D. Y., et al. (2007). Use of the Electrical Aerosol Detector as an Indicator of the Surface Area of Fine Particles Deposited in the Lung. *Journal of Air & Waste Management Association, 57*, 211-220.

# REPORT DOCUMENTATION PAGE

*Form Approved*
*OMB No. 074-0188*



| **1. REPORT DATE** *(DD-MM-YYYY)* | **2. REPORT TYPE** | **3. DATES COVERED** *(From – To)* |
|---|---|---|
| 24-03-2011 | Master's Thesis | Oct 2009 – Mar 2011 |

**4. TITLE AND SUBTITLE**

Characterization of Graphite Composite Material Particulates from United States Air Force Aircraft Maintenance Operations

**5a. CONTRACT NUMBER**

**5b. GRANT NUMBER**

**5c. PROGRAM ELEMENT NUMBER**

**6. AUTHOR(S)**

Yon, Richard E., Capt, USAF

**5d. PROJECT NUMBER**
NONE

**5e. TASK NUMBER**

**5f. WORK UNIT NUMBER**

**7. PERFORMING ORGANIZATION NAMES(S) AND ADDRESS(S)**

Air Force Institute of Technology
Graduate School of Engineering and Management (AFIT/EN)
2950 Hobson Way
WPAFB OH 45433-7765

**8. PERFORMING ORGANIZATION REPORT NUMBER**

AFIT/GIH/ENV/11-M04

**9. SPONSORING/MONITORING AGENCY NAME(S) AND ADDRESS(ES)**
United States Air Force School of Aerospace Medicine
Attn: Lt Col Darrin Ott
Kettering Business Park
1050 Forrer Blvd
Kettering, OH 45420
Darrin.Ott@wpafb.af.mil, (DSN 986-8555)

**10. SPONSOR/MONITOR'S ACRONYM(S)**
USAFSAM/OEHR

**11. SPONSOR/MONITOR'S REPORT NUMBER(S)**

**12. DISTRIBUTION/AVAILABILITY STATEMENT**
APPROVED FOR PUBLIC RELEASE; DISTRIBUTION UNLIMITED.

**13. SUPPLEMENTARY NOTES**
This material is declared a work of the U.S. Government and is not subject to copyright protection in the United States.

**14. ABSTRACT**
Due to the benefits of their material properties, advanced composite materials (ACM) are increasingly being used as structural components on aircraft, especially within the United States Air Force. As a result, the potential exists for occupational exposures to structural maintenance employees while repairing and fabricating aircraft components. Two field studies were conducted for this thesis in order to characterize ACM aerosol size distribution, determine the feasibility of utilizing direct reading instruments (DRIs) in the field, and ensure workers are protected with adequate controls. In order to characterize exposure, traditional integrated air sampling and DRIs were positioned together near an ACM panel being fabricated. Gravimetric analyses and fiber counts were conducted on the integrated samples, whereas particle counts and size distributions were analyzed using the DRIs (optical and condensation particle counters). The second field study involved utilizing the DRIs during a C-17 crash and recovery operation, which confirmed they can be helpful for base-level bioenvironmental engineers (BEEs) for recommending personal protective equipment for the clean-up crew. The results of this research suggest that the combination of an OPC and a CPC enable the creation of one particle size distribution that can be used for ensuring adequacy of engineering controls.

**15. SUBJECT TERMS**
Graphite Composite, Industrial Hygiene, Aerosol, Carbon Fiber, Particle Characterization

| **16. SECURITY CLASSIFICATION OF:** | | | **17. LIMITATION OF ABSTRACT** | **18. NUMBER OF PAGES** | **19a. NAME OF RESPONSIBLE PERSON** |
|---|---|---|---|---|---|
| **a. REPORT** | **b. ABSTRACT** | **c. THIS PAGE** | | | Dirk P. Yamamoto, Lt Col, USAF (ENV) |
| U | U | U | UU | 100 | **19b. TELEPHONE NUMBER** *(Include area code)*<br>(937) 255-3636, ext 4511;<br>e-mail: Dirk.Yamamoto@afit.edu |

**Standard Form 298 (Rev. 8-98)**
Prescribed by ANSI Std. Z39-18

*Form Approved*
*OMB No. 074-0188*